Scaling and universality in the spanning probability for percolation

J.-P. Hovi[1,2] and Amnon Aharony[1,3]
[1]*Raymond and Beverly Sackler Faculty of Exact Sciences, School of Physics and Astronomy, Tel Aviv University, Ramat Aviv 69978, Tel Aviv, Israel*
[2]*Laboratory of Physics, Helsinki University of Technology, 02150 Espoo, Finland*
[3]*Department of Physics, University of Oslo, Oslo, Norway*
(Received 5 September 1995)

We discuss the spanning percolation probability function for three different spanning rules, in general dimensions, with both free and periodic boundary conditions. Our discussion relies on the renormalization group theory, which indicates that, apart from a few scale factors, the scaling functions for the spanning probability are determined by the fixed point and therefore are universal for every system with the same dimensionality, spanning rule, aspect ratio, and boundary conditions. For square and rectangular systems, we combine this theory with simple relations between the spanning rules and with duality arguments, and find strong relations among different derivatives of the spanning function with respect to the scaling variables, thus yielding several universal amplitude ratios and allowing a systematic study of the corrections to scaling, both singular and analytic, in the system size. The theoretical predictions are numerically confirmed with excellent accuracy.

PACS number(s): 64.60.Ak, 05.70.Jk

I. INTRODUCTION

The function $R(p, L)$, giving the probability for a finite dilute system of size L to span (or percolate) at (site or bond) occupancy p, arises naturally in the context of the real-space renormalization group (RSRG) approach. This approach is based on partitioning the underlying lattice into cells of size b and replacing all b^d sites by a single supersite. Reynolds *et al.* [1] studied the one-parameter approximation of the renormalization group (RG) transformation, which declares the supersite occupied if there exists a percolating cluster spanning the original cell. In this approximation, the renormalized cell has occupancy $p' = R(p, b)$. This approximation led to good quantitative results concerning the numerical values of the percolation threshold and provided excellent approximations to the critical exponents. However, this approximate RSRG calculation yielded $R(p_c, \infty) = p_c$ and therefore this quantity was thought to be nonuniversal.

The study concerning the universal aspects of the spanning probability function was initiated by Langlands *et al.* [2]. This work dealt with the spanning of rectangular systems and showed numerically that the spanning probability for the infinite system at the critical threshold is a universal function of the aspect ratio of the rectangle. Inspired by these numerical results Cardy [3] derived an analytical formula for this function using the conformal invariance of the spanning probability in two-dimensional (2D) percolation. This formula agreed with numerical results for various 2D percolation problems in Ref. [2]. The latter authors later generalized the analytical formula for other shapes (e.g., parallelograms [4]) and found good agreement betweeen the numerical evidence and analytical predictions from the conformal invariance, confirming, in particular, the universality of the spanning probability as a function of the aspect ratio also for these other shapes [4].

Working independently, Grassberger [5] found that for the site problem on the square lattice, with spanning defined according to the rule $\mathfrak{R}_1$ of Ref. [1] (spanning in one given direction, free boundaries in the other direction), the numerical evidence supports that $R(p_c, \infty) = 1/2 \neq p_c$. He also pointed out that this value is consistent with the bond problem for which $R(p_c, L) = 1/2$ for every L [6], indicating universality. The spanning probability for the site problem was subsequently studied with better numerical accuracy by Ziff [7], who reconfirmed $R(p_c, \infty) = 1/2$ and argued that while this value is consistent with universality with the bond problem, the result contradicts the RG theory because the approximate RG transformation of Ref. [1] would imply that $R(p_c, \infty) = p_c \neq 1/2$. In the work accounting for our early results [8], we pointed out that this apparent nonuniversal $R(p_c, \infty)$ in the RG of Ref. [1] is an artifact of the naive application of the one-parameter approximation of the RG transformation and showed that a correct application of the RG theory implies not only that $R(p_c, \infty)$ is generally universal, but also gives that $R(p_c, \infty) = 1/2$ *exactly* for rule $\mathfrak{R}_1$ on the square systems [9], in agreement with the results from the conformal field theory [3,2,4]. Further discussion of the approximate RSRG is given in Appendix A.

Having identified the universal spanning probability as a characteristic of the fixed point of the RG transformation, one is well motivated to start asking questions about the scaling behavior of this function, for finite $p - p_c$ and L. It is well understood [10] that near the critical point the spanning probability depends on the scaling variable $(p - p_c)L^{1/\nu}$. Subsequently Ziff [7] made attempts to study the scaling behavior of the function $R(p_c, L)$ be-

yond the one-parameter approximation by introducing an analytical finite-size correction (proportional to $1/L$) to the spanning probability function. We criticized and generalized this approach [8] by arguing that, in fact, for p near p_c one should expect $R(p, L)$ also to depend on the infinite number of the irrelevant variables $\{\omega_i\}$, which give rise to nonanalytic corrections proportional to $\{L^{-\theta_i}\}$. In 2D percolation, the leading correction to scaling has $\theta_1 \approx 0.85$ [11], which should generally dominate the finite-size correction for large L.

Our application of the RG theory [8] also gave a number of predictions concerning universality and scaling in percolation, containing, in particular, predictions concerning several universal amplitude ratios. Those predictions were checked for different 2D lattices against our preliminary data in Ref. [8]. While these universal amplitude ratios are not restricted to two dimensions, this inspired several papers, which checked and verified our predictions also in higher dimensions [12,13].

During this process Gropengiesser and Stauffer [13] found out that different boundary conditions yield different values for the spanning probability at criticality. Recently, Hu [14] also studied the spanning probability for free and periodic boundary conditions and noticed that different boundary conditions give different scaling functions near the critical region. In fact, similar behavior is known [15] to occur for the Ising model, which has different scaling functions for free and periodic boundary conditions, while the critical point and the critical exponents remain unchanged. Very recently, Hu and Chen [16] have also studied the bond problem on a honeycomb lattice of rectangular shape and found that different aspect ratios give different scaling functions.

In this paper we employ and study the machinery of Ref. [8] in more detail. We present a theory for the spanning probability, valid in general dimensions, which treats systematically the corrections to scaling and explains, e.g., the previous findings of Refs. [13,14,16]. Our approach relies on the general result from the RG that the scaling functions are universal [17,18,8], reflecting the fact that close to p_c all the percolation problems look similar. The scaling variables appear in the scaling functions together with nonuniversal metric factors [19].

However, we find that these scaling functions *do depend* on the *physical question* we pose, i.e., they depend on the shape of the system, boundary conditions, and spanning rules, but *not* on the lattice connectivity. This can indeed be expected from the RG theory because all the scaling functions are determined by the physical question one asks at the RG fixed point. The fixed point, which lies in the many-dimensional space of the coupling constants, is the same for all the problems with the same dimensionality but arbitrary finite-range connectivity. These statements already explain the different scaling functions [giving also different values for $R(p_c, \infty)$ [13]] for various boundary conditions [14] and aspect ratios [16].

In other words, the spanning rule, boundary condition, and system shape each corresponds to an additional variable. The spanning probability is ultimately a universal function of all these variables. Following Langlands *et al.* [2,4] we are able to consider the universal dependence of the spanning probability on the additional variable representing the aspect ratio of the rectangular system [9]. We also discuss the dependence on the spanning rule and boundary conditions.

Although we present numerical results for 2D percolation, our approach yields several predictions, which are valid in general d dimensions: $R(p_c, \infty)$ is not necessarily equal to p_c, but is a universal number; the universality of the scaling function is manifested through universal amplitude ratios. We also predict that with fixed occupancy p and for the spanning rule $\mathfrak{R}_1$, the spanning probability in d dimensions scales as $R(L) = [a_-(p)]^L$ for all $p < p_c$ and $[1-R(L)] = [a_+(p)]^{L^{d-1}}$ for $p > p_c$ (see Appendix B).

The rest of the paper is organized as follows. In Sec. II we give a general scaling theory for the spanning probability function. These general principles are then applied for 2D percolation in Sec. III. First (see Sec. III A), working specifically with 2D square systems with free boundaries, we find that the scaling functions have to obey several conditions arising from duality arguments and from sum rules that connect different spanning rules. Due to the universality of the scaling function, these restrictions force several derivatives of the scaling function to vanish and this simplifies the expansion as a power series in the scaling variables that represent irrelevant fields in the RG sense. We find that for systems that obey duality, the metric factors for the scaling variables do not depend on the spanning rule. The power series expansion makes it possible to check numerically several universal amplitude ratios. Extending the discussion to rectangular systems (see Sec. III C), we write the spanning probability as a universal function of $(p - p_c)$, $\{\omega_i\}$, and the aspect ratio, which gives again several universal amplitude ratios. At the end of Sec. III, similar predictions are worked out for periodic boundary conditions (Sec. III D). Numerical verifications of the various theoretical predictions are presented in Sec. IV. Finally, a short conclusion completes the paper in Sec. V.

II. SCALING THEORY FOR THE SPANNING PROBABILITY

In this section we study the general properties of the spanning probability function $R(p, L)$, which is the probability that a finite cell of size L spans at occupancy p. The main result of this section is that the spanning probability is a universal function of the scaling variables for given dimension, spanning rule, boundary condition, and system shape, but independent of lattice structure and (finite) interaction range. It directly follows that the spanning probability at criticality is a universal number.

A. Scaling relations

Near the critical point the spanning probability function depends on the scaling variables, including $t = (p - p_c)$, the system size L, and the irrelevant variables $\{\omega_i\}$ $(i = 1, 2, \ldots)$,

$$R(p,L) = \tilde{F}(At, \{B_i\omega_i\}, L), \tag{1}$$

where A and B_i, which make the arguments of the function $\tilde{F}$ dimensionless, are nonuniversal metric factors [19,18]. One expects that the metric factors A and B_i are the only nonuniversal system-dependent parameters entering the universal scaling functions because the metric factor for the system size can be set to unity by a suitable choice of A and B_i. After choosing the metric factors, the function $\tilde{F}$ is universal, i.e., it is the same for all problems with the same dimension, spanning rule, aspect ratio, and boundary conditions.

Upon the renormalization transformation with the length rescale factor b, the scaling variables are expected to obey the linearized recursion relations

$$t' = b^{1/\nu}t, \tag{2}$$

$$\omega_i' = b^{-\vartheta_i}\omega_i, \tag{3}$$

$$L' = b^{-1}L, \tag{4}$$

where the scaling powers are written in terms of the correlation length exponent ν and the correction to scaling exponents $\vartheta_i > 0$. In particular, in two-dimensional percolation one has $\nu = 4/3$ and the leading irrelevant scaling field has $\vartheta_1 \approx 0.85$ [11]. Equations (2) and (4) are the origin of finite-size scaling.

In addition to the irrelevant scaling fields, we have to deal with the finite-size corrections. The leading finite-size correction depends most strikingly on the boundary conditions of the system. It is plausibly expected that the leading finite-size correction to R in the systems with *free* boundaries is of the order $1/L$, which is also numerically confirmed by Ziff [7]. This kind of a correction arises, e.g., if the variable L in $\tilde{F}$ should be replaced by $L + a$ due to the free boundaries. On the other hand, for *periodic* boundary conditions we expect that the $1/L$ correction vanishes because a shift in the boundaries just translates the system without affecting the system size.

These finite-size corrections can be brought into the scaling framework [Eq. (1)] by treating them as "irrelevant fields" with $\vartheta_2 = 1$. In what follows we append the finite-size corrections together with the correction terms ω_i arising from the irrelevant scaling fields. We shall later check the similarities and the differences between these two types of corrections. One should also be aware that further contributions to the scaling function may arise from nonlinear scaling fields [20], but these terms are ignored in the present treatment.

B. Scaling function for the spanning probability

Renormalizing the system with the length rescale factor b and with the help of the recursion relations Eqs. (2)–(4), we find that for given spanning rule, boundary conditions, and aspect ratio,

$$\begin{aligned} R(p,L) &= \tilde{F}(At, \{B_i\omega_i\}, L) \\ &= \tilde{F}(Atb^{1/\nu}, \{B_i\omega_i b^{-\vartheta_i}\}, L/b) \\ &= \tilde{F}(Atb^{l/\nu}, \{B_i\omega_i b^{-l\vartheta_i}\}, L/b^l). \end{aligned} \tag{5}$$

Ignoring the transient steps and close to p_c, we may renormalize the system until $L = b^l$ [10], which yields

$$\begin{aligned} R(p,L) &= \tilde{F}(AtL^{1/\nu}, \{B_i\omega_i L^{-\vartheta_i}\}, 1) \\ &\equiv F(AtL^{1/\nu}, \{B_i\omega_i L^{-\vartheta_i}\}) \\ &\equiv F(Ax, \{B_i y_i\}) \equiv F(\hat{x}, \{\hat{y}_i\}), \end{aligned} \tag{6}$$

where we have defined $x = tL^{1/\nu}$, $\hat{x} = Ax$, $y_i = \omega_i L^{-\vartheta_i}$, and $\hat{y}_i = B_i y_i$ $(i = 1, 2, \ldots)$. This equation gives the general scaling form for the spanning probability in terms of the *universal* scaling function $F(\hat{x}, \{\hat{y}_i\})$ and *nonuniversal* metric factors A and B_i.

The universality of F immediately implies that $R(p = p_c, L \to \infty) = F(0,0)$ is universal (for given spanning rule, boundary conditions, and aspect ratio) *independent of the metric factors.* However, the derivative of F with respect to x obeys $\frac{\partial F}{\partial x} = A\frac{\partial F}{\partial \hat{x}}$ and therefore we have the freedom to set $\frac{\partial F}{\partial \hat{x}} = 1$ at $x = y_i = 0$ for one specific problem on a particular lattice and thus fix A for that system. Having chosen A that way, all other scaling functions will be universal functions of $\hat{x} = Ax$, with no further choice of scales [17]. Thus, if we now change the problem (e.g., from periodic to free boundaries), then the new function $F_{\rm new}$ is a universal function of $\hat{x} = Ax$, with the *same* scale factor A. Specifically, we expect $\frac{\partial F_{\rm new}}{\partial \hat{x}}|_{x=y_i=0} = \frac{1}{A}\frac{\partial F_{\rm new}}{\partial x}|_{x=y_i=0}$ to be universal.

An alternative approach, which we adopt below, is to set a different scale factor for each problem, e.g., $A_{\rm new}$ for the latter case, such that $\frac{\partial F_{\rm new}}{\partial \hat{x}_{\rm new}}|_{x=y_i=0} = \frac{1}{A_{\rm new}}\frac{\partial F_{\rm new}}{\partial x}|_{x=y_i=0} = 1$. Universality then implies that $A_{\rm new}/A = \frac{\partial F_{\rm new}}{\partial \hat{x}}|_{x=y_i=0}$ is also universal. Similar rules, involving $\frac{\partial F}{\partial \hat{y}_i}|_{x=y_i=0}$, are used to set the (now problem-dependent) metric factors $\{B_i\}$.

The universality of $R(p_c, \infty)$ immediately implies that it need not be equal to p_c [7]. This becomes readily apparent from our RG formulation, which treats the irrelevant scaling variables in a systematic way. In fact, one can show that $R(p_c, L \to \infty) \neq p_c$ also within the one-parameter approximation [1] of the RG transformation (see Appendix A). When carefully applied, the one-parameter approximation can also be used to extract useful information concerning, e.g., the scaling of the spanning probability at a fixed occupancy (see Appendix B).

III. SPANNING PROBABILITY IN 2D PERCOLATION

Up to this point, our results are very general and apply at any dimension, spanning rule, boundary conditions, etc. From now on we restrict ourselves to 2D percolation.

A. Different spanning rules for square systems with free boundaries

In their seminal papers (see Ref. [1] and also references therein) Reynolds *et al.* discussed three different rules, denoted by $\mathfrak{R}_0$, $\mathfrak{R}_1$, and $\mathfrak{R}_2$, for spanning a cell

of size b using free boundary conditions. These rules state that the cell percolates if there exists a cluster that for $\mathfrak{R}_0$ spans the cell either horizontally or vertically, for $\mathfrak{R}_1$ spans the lattice in one given direction (say, horizontally), and for $\mathfrak{R}_2$ spans the cell in both directions. Each of these rules involves a different scaling function $F_r(A_r x, B_{i,r} y_i)$, $r = 0, 1, 2$, with different limiting values $F_r(0,0)$. However, all the scaling functions are determined by the RG fixed point. As mentioned above, our convention also allows for different metric factors for each rule.

In this section we study the relations among the scaling functions and metric factors. We find that sum rules, arising from the definitions of the spanning, and duality arguments give powerful relations between the derivatives of the functions F_r. This simplifies the expansion of the scaling functions as power series in the scaling variables. These series are employed in the numerical studies.

1. Sum rules

The three spanning rules are not completely independent of each other. Using elementary algebra of probabilities one finds that the probability to span the cell in either direction (F_0) is equal to the probability to span the cell horizontally (F_1) plus the probability for vertical spanning (F_1), minus the probability for spanning the cell in both directions (F_2) [1]. This gives the connection between the three scaling functions

$$F_0(A_0 x, \{B_{i,0} y_i\}) = 2F_1(A_1 x, \{B_{i,1} y_i\}) - F_2(A_2 x, \{B_{i,2} y_i\}). \quad (7)$$

At the fixed point, $x = L^{1/\nu}(p - p_c) = 0$ and $y_i = \omega_i L^{-\vartheta_i} = 0$ and we find that

$$F_0(0,0) = 2F_1(0,0) - F_2(0,0), \quad (8)$$

relating the universal limits for different spanning rules.

Equation (7) also reveals connections among the scale factors for the different spanning rules. Taking the derivative of Eq. (7) with respect to x and evaluating the derivatives at criticality, we find

$$A_0 \frac{\partial F_0}{\partial \hat{x}}(0,0) = 2A_1 \frac{\partial F_1}{\partial \hat{x}}(0,0) - A_2 \frac{\partial F_2}{\partial \hat{x}}(0,0), \quad (9)$$

where all the derivatives of the universal scaling functions are also universal numbers. Supposing that all of them are nonzero, one may normalize the scale factors by setting $\frac{\partial F_0}{\partial \hat{x}}(0,0) = \frac{\partial F_1}{\partial \hat{x}}(0,0) = \frac{\partial F_2}{\partial \hat{x}}(0,0) = 1$, which gives a sum rule

$$A_0 = 2A_1 - A_2 \quad (10)$$

and confirms that ratios A_j/A_k are universal. Similarly, we find the relation between the amplitudes $B_{i,r}$,

$$B_{i,0}\Delta_{i,0} = 2B_{i,1}\Delta_{i,1} - B_{i,2}\Delta_{i,2}\ , \quad (11)$$

where $\Delta_{i,r} = \frac{\partial F_r}{\partial \hat{y}_i}(0,0)$ are universal numbers, which may also be zero.

2. Duality and its consequences

If we use free boundary conditions, further information can be extracted by considering two dual lattices, e.g., square lattices with nearest-neighbor (NN) and $NN+$ next-nearest-neighbor (NNN) connectivity. Then one has [1]

$$R_1(p,L) + R'_1(q,L) = 1, \quad (12)$$
$$R_0(p,L) + R'_2(q,L) = 1, \quad (13)$$

where primed quantities refer to the dual lattice, which has occupancy $q = 1-p$ and $q_c = 1-p_c$. Using the universality of the spanning probability function, which gives that R_r and R'_r are equal to the same scaling function F_r, and noting that $x' = L^{1/\nu}(q-q_c) = L^{1/\nu}[1-p-(1-p_c)] = -x$, one may rewrite the previous equations in the form

$$F_1(A_1 x, \{B_{i,1} y_i\}) + F_1(-A'_1 x, \{B'_{i,1} y_i\}) = 1, \quad (14)$$
$$F_0(A_0 x, \{B_{i,0} y_i\}) + F_2(-A'_2 x, \{B'_{i,2} y_i\}) = 1. \quad (15)$$

We emphasize that these relations *do not hold* if one uses periodic boundary conditions for the spanning because there is no duality between these lattices in that case (see Sec. III D).

We can now proceed as before. Substituting $x = y_i = 0$ in Eq. (14) yields directly the result for the spanning probability in a square system according to the rule $\mathfrak{R}_1$,

$$F_1(0,0) = \frac{1}{2}. \quad (16)$$

Similarly, the corresponding probabilities are complementary for rules $\mathfrak{R}_0$ and $\mathfrak{R}_2$,

$$F_0(0,0) + F_2(0,0) = 1. \quad (17)$$

Taking the derivative with respect to x or y_i and evaluating the derivatives at $x = y_i = 0$, we find that amplitudes for dual lattices satisfy

$$A_1 = A'_1, \quad (18)$$
$$A_0 = A'_2, \quad (19)$$
$$B_{i,1}\Delta_{i,1} = -B'_{i,1}\Delta_{i,1}, \quad (20)$$
$$B_{i,0}\Delta_{i,0} = -B'_{i,2}\Delta_{i,2}. \quad (21)$$

For a self-dual system, such as the bond problem on the square lattice, Eq. (20) implies that

$$B_{i,1}\Delta_{i,1} = 0. \quad (22)$$

On the other hand, the ratios between the metric factors for the irrelevant fields are expected to be universal, which is plausible only if $\Delta_{i,1} = 0$, otherwise $B_{i,1} = 0$ for all the lattices. As we discuss below, this condition need not apply to the $1/L$ finite-size corrections. In what follows we therefore set $\Delta_{i,1} = 0$ for the irrelevant fields.

The universal ratios for the metric factors are set by choosing $\Delta_{i,0} = \Delta_{i,2} = 1$, when Eq. (21) gives

$$B_{i,0} = -B'_{i,2}. \tag{23}$$

Continuing to take higher derivatives, we realize that the dual properties [Eqs. (14) and (15)] give powerful relations between the derivatives of the scaling functions:

$$D^n F_1(A_1 x, \{B_{i,1} y_i\}) = (-1)^{n+1} D^n F_1(-A_1 x, \{-B_{i,1} y_i\}), \tag{24}$$

$$D^n F_0(A_0 x, \{B_{i,0} y_i\}) = (-1)^{n+1} D^n F_2(-A_0 x, \{-B_{i,0} y_i\}), \tag{25}$$

where $D^k = \frac{\partial^k}{\partial \hat{x}^{k_0} \partial \hat{y}_1^{k_1} \ldots}$, $k = \sum_j k_j$, and $n = 1, 2, \ldots$. In particular, Eq. (25) implies that $D^n F_1(\hat{x}, \{\hat{y}_i\})$ is an even (odd) function of both its variables for odd (even) n. Specifically, this implies that

$$D^{2n} F_1(0,0) = 0. \tag{26}$$

Similarly,

$$D^n F_0(0,0) = (-1)^{n-1} D^n F_2(0,0). \tag{27}$$

We can use the information of Eqs. (26) and (27) together with the general sum rule of Eq. (7). A second derivative of Eq. (7) with respect to x, combined with Eq. (26), yields

$$(A_0^2 - A_2^2) \frac{\partial^2 F_0}{\partial \hat{x}^2} = 0. \tag{28}$$

Thus we find $A_0 = A_2$, consistent with Eq. (19) for self-dual lattices. Combining this with Eq. (10) implies that, in fact, the amplitudes for different rules are all equal $A_0 = A_1 = A_2 \equiv A$. We shall see below that equal amplitudes are indeed confirmed numerically. Thus the universal ratios A_j/A_k are all equal to one.

Similarly, taking derivatives of Eq. (7) and using Eqs. (26) and (27), we find

$$A^l [B_{i,0}^m - B_{i,2}^m] D^{l+m} F_0(0,0) = 0 \quad \text{for } l+m \text{ even}, \tag{29}$$

$$A^l [B_{i,0}^m + B_{i,2}^m] D^{l+m} F_0(0,0) = 2A^l B_{i,1}^m D^{l+m} F_1(0,0) \quad \text{for } l+m \text{ odd}. \tag{30}$$

Due to the universal ratios between the metric factors, these equations imply that

$$B_{i,0} = -B_{i,2}, \tag{31}$$

consistently with Eq. (22) for self-dual lattices. Furthermore, we find that

$$D^{l+m} F_1(0,0) = 0 \quad \text{for even } l, \text{ odd } m, \tag{32}$$

$$D^{l+m} F_0(0,0) = 0 \quad \text{for } l, m \text{ odd}. \tag{33}$$

Combining Eqs. (32) and (26) we find that actually *all the derivatives of F_1 taken with respect to irrelevant variables at $x = y_i = 0$ vanish* and therefore $R(p_c, L)$ does not depend on y_i.

At this point it is important to distinguish the irrelevant scaling fields and the finite-size corrections. The argument leading to Eq. (22) is exact for both kinds of corrections in *self-dual* systems. However, extending this condition for other systems, which are not self-dual, relies on the universality between the ratios of the metric factors. This latter condition must hold *only* for the corrections due to the irrelevant scaling fields. Therefore, Eqs. (22) and (31)–(33) are expected to hold generally for irrelevant fields, but the finite-size corrections obey only the weaker condition Eq. (11). In particular, $R(p_c, L)$ may still depend on the finite-size correction $1/L$.

Collecting all this information together, one finds the expansions of the spanning probability function near the fixed point. Expanding in powers of y_i, rule $\mathfrak{R}_1$ gives

$$F_1(Ax, \{B_{i,1} y_i\}) = \frac{1}{2} + f_1^1(Ax) + \sum_i [(B_{i,1} y_i) f_{2i}^1(Ax)] + \sum_{i,j} [(B_{i,1} y_i)(B_{j,1} y_j) f_{3ij}^1(Ax)] + \cdots, \tag{34}$$

where the functions f are defined by

$$f_1^r(Ax) = F_r(Ax, \{B_{i,1} y_i = 0\}) - F_r(0, \{B_{i,1} y_i = 0\}), \tag{35}$$

$$f_{Nijk\ldots}^r(Ax) = \frac{1}{(N-1)!} \frac{\partial^{N-1} F_r}{\partial \hat{y}_i \partial \hat{y}_j \partial \hat{y}_k \cdots} (Ax, \{B_{i,1} y_i = 0\}) \quad \text{for } N > 1. \tag{36}$$

The discussion above implies that f_1^1 and f_{3ij}^1 are odd functions, while f_{2i}^1 are even [8], and $f_{Nijk\ldots}^1(0) = 0$ for the irrelevant fields.

The other two rules can be expanded similarly. For example, rule $\mathfrak{R}_0$ gives

$$F_0(Ax, \{B_{i,0} y_i\}) = F_0(0,0) + f_1^0(Ax) + \sum_i [(B_{i,0} y_i) f_{2i}^0(Ax)] + \sum_{i,j} [(B_{i,0} y_i)(B_{j,0} y_j) f_{3ij}^0(Ax)] + \cdots, \tag{37}$$

where $f_1^0(0) = 0$ and the $[f_{2i}^0(\hat{x})]$ are even functions for the irrelevant fields.

B. Predictions for square systems with free boundaries

In this section we discuss the consequences of the expansions of the spanning probability near the critical

point. We can check these expansions studying the function F_r numerically at p_c as a function of the cell size L [7]. On the other hand, since $\frac{dR_L(p)}{dp}$ gives the probability distribution for a finite system of size L to span for the first time at occupancy p [10], we can alternatively study the central moments of this distribution [23]

$$\mu_n = \int dp(p-p_c)^n \frac{dR_L(p)}{dp}, \tag{38}$$

$n = 1, 2, \ldots$. As will be explained in the next section, the derivative $\frac{dR_L}{dp}$ is calculated numerically for a set of discrete values of p, which gives a histogram $\frac{\Delta R_L}{\Delta p}(p_i)$ representing the derivative [10]. The histogram is properly normalized such that $\sum_i \frac{\Delta R_L}{\Delta p}(p_i) = 1$. The moments are then calculated using $\mu_n \approx \sum_i (p_i - p_c)^n \frac{\Delta R_L}{\Delta p}(p_i)$.

In the numerical work we expect that as the system size L gets large, the behavior of the spanning probability function can be characterized by the leading (non-analytic) correction ϑ_1 due to the irrelevant scaling fields (confluent corrections) and by the analytical correction $\vartheta_2 = 1$ from the finite-size corrections. The leading non-analytic correction has been given in the literature [11], and we expect $\vartheta_1 \approx 0.85$.

Let us concentrate first on the rule $\mathfrak{R}_1$. As discussed after Eq. (32), $R(p_c, L)$ does not depend on the irrelevant scaling fields $\{\omega_i\}$. However, this does not exclude the finite-size corrections, of order $1/L$, for the case of free boundaries. In that case we have

$$F_1(0, \{B_i y_i\}) \approx 1/2 + a_1 L^{-\vartheta_2}, \quad \vartheta_2 = 1, \tag{39}$$

and Eq. (22) gives that $a_1 = 0$ for self-dual systems. This result gives the theoretical basis for Ziff's [7] finite-size scaling form for these systems. In fact, it follows from the universality with the self-dual lattices.

Since $f_1^1(\hat{x})$ and $f_{3ij}^1(\hat{x})$ are odd, Eq. (34) implies that the nth moment for rule $\mathfrak{R}_1$, $\mu_{1,n} = \int dp(p-p_c)^n \frac{dF_1}{dp}$, multiplied by $(AL^{1/\nu})^n$ scales as

$$\hat{\mu}_{1,n} \equiv (AL^{1/\nu})^n \mu_{1,n} = \int d\hat{x}\hat{x}^n \frac{dF_1}{d\hat{x}}$$
$$= \begin{cases} d_{n,10}L^{-\vartheta_1} + d_{n,01}L^{-\vartheta_2} + O(L^{-\vartheta_3}) & \text{for } n, k+l = \text{ odd} \\ d_{n,00} + d_{n,20}L^{-2\vartheta_1} + d_{n,11}L^{-\vartheta_1-\vartheta_2} + d_{n,02}L^{-2\vartheta_2} + O(L^{-\vartheta_3}) & \text{for } n, k+l = \text{ even}, \end{cases} \tag{40}$$

where

$$d_{n,kl} = (B_1\omega_1)^k (B_2\omega_2)^l \frac{1}{k!l!} \times \int d\hat{x}\hat{x}^n \frac{\partial}{\partial \hat{x}} \frac{\partial^{k+l} F_1}{\partial \hat{y}_1^k \partial \hat{y}_2^l}(\hat{x}, \{\hat{y}_i = 0\}). \tag{41}$$

Equation (40) reveals that as $L \to \infty$ the odd (scaled) moments vanish, but even scaled moments approach nonzero values. The coefficients $\{d_{n,kl}\}$ are proportional to the amplitudes for the correction terms. In particular, comparing $L^{n/\nu}\mu_{1,n} = A^{-n} d_{n,00}$ between different rules as depicted below, we can check the prediction that the amplitudes A are independent of the spanning rule.

In addition, Eq. (40) also gives a very important prediction concerning the moment ratios. As $L \to \infty$, the moment ratios $\mu_n/\mu_2^{(n/2)}$ for even n depend only on the universal scaling function and therefore they are expected to be universal. These moment ratios are easy to study numerically and therefore we have concentrated on them, but in addition to that there exists an infinite number of universal ratios between the correction terms $\{d_{n,kl}\}$, e.g., $d_{n,k0}/(d_{n,10})^k$.

The other two rules obey similar expansions. First, the spanning probability at the critical threshold can be expanded as

$$F_0(0, \hat{y}_i) = F_0(0,0) + b_1^0 L^{-\vartheta_1} + a_0/L + b_2^0 L^{-2\vartheta_1} + \cdots, \tag{42}$$

$$F_2(0, \hat{y}_i) = [1 - F_0(0,0)] + b_1^2 L^{-\vartheta_1} + a_2/L + b_2^2 L^{-2\vartheta_1} + \cdots, \tag{43}$$

where

$$b_k^r = (B_1\omega_1)^k \frac{1}{k!} \frac{\partial^k F_r}{\partial \hat{y}_1^k}(0,0), \tag{44}$$

$b_1^0 = -b_1^2$, and $a_0 = 2a_1 - a_2$ [see Eq. (39)]. For these spanning rules the irrelevant scaling fields should be present even at p_c. The main point in Eq. (44) is that although the b_k^r's are not universal, the *ratios* $b_k^r/(b_1^r)^k$ involve only the derivatives of the universal scaling function and should therefore also be *universal*. However, in addition to the finite-size corrections, higher-order scaling fields give contributions proportional to $L^{-\vartheta_3}$, with ϑ_3 apparently of order 2, thus making the numerical confirmation of these universal amplitude ratios very difficult. The universal amplitude ratios for the irrelevant variables are more easily seen in the case of periodic boundary conditions (see Secs. III D and IV).

Second, the scaled moments are given by

$$\hat{\mu}_{0,n} \equiv (AL^{1/\nu})^n \mu_{0,n} = e_{n,0} + \sum_{k,l} e_{n,kl} L^{-k\vartheta_1 - l\vartheta_2} + \cdots, \tag{45}$$

$$\hat{\mu}_{2,n} \equiv (AL^{1/\nu})^n \mu_{2,n} = (-1)^n \left(e_{n,0} + \sum_{k,l} e_{n,kl} L^{-k\vartheta_1 - l\vartheta_2} + \cdots \right), \quad (46)$$

where the $\{e_{n,kl}\}$'s are analogous to the $\{d_{n,kl}\}$'s,

$$e_{n,kl} = (B_1\omega_1)^k (B_2\omega_2)^l \frac{1}{k!l!} \times \int d\hat{x}\hat{x}^n \frac{\partial}{\partial \hat{x}} \frac{\partial^{k+l} F_0}{\partial \hat{y}_1^k \partial \hat{y}_2^l}(\hat{x}, \{\hat{y}_i = 0\}). \quad (47)$$

The moment ratios μ_n/μ_1^n depend only on the universal scaling function and are thus universal. Furthermore, as before, with extremely good data one could also check and verify the universal ratios between the $\{e_{n,kl}\}$'s [e.g., $e_{n,k0}/(e_{n,10})^k$].

Because the amplitudes A are found to be equal for all the rules, we expect from Eq. (7) that as $L \to \infty$ the scaled moments also obey the sum rule $\hat{\mu}_{0,n} = 2\hat{\mu}_{1,n} - \hat{\mu}_{2,n}$ and, in fact, $d_{n,00} = e_{n,00}$ for even n. These predictions are equivalent to equal A's for different rules.

C. Rectangular systems with free boundaries

In this section we extend the discussion above to rectangles [9], which have recently been studied by Langlands *et al.* [2,4] and Cardy [3], who used arguments based on conformal mappings. In particular, Cardy derived an analytical formula for the spanning probability for the infinite rectangular system with $\mathfrak{R}_1$. Here we also concentrate on rule $\mathfrak{R}_1$.

Define the aspect ratio r for a rectangular lattice of width L and height H by $r = H/L$. The amplitudes for the variables $t, \{\omega_i\}$ are expected to remain unchanged and all our earlier results should emerge by setting $r = 1$. We start by looking at the function F^- (F^+), which is the probability for the horizontal spanning for $r \geq 1$ ($r < 1$). Thus the spanning probability function is given by

$$F^{\pm} = \tilde{F}^{\pm}(At, \{B_i\omega_i\}, L, H) \quad (48)$$

$$= \tilde{F}^{\pm}(Atb^{1/\nu}, \{B_i\omega_i b^{-\vartheta_i}\}, L/b, H/b), \quad (49)$$

where the last equality follows from rescaling with b. If $r \geq 1$, we can set $b = L$ and have

$$F^-(p, L, r) = \tilde{F}^-(AtL^{1/\nu}, \{B_i\omega_i L^{-\vartheta_i}\}, 1, r). \quad (50)$$

If $r < 1$, we can set $b = H$ and find

$$F^+(p, L, r) = \tilde{F}^+(AtH^{1/\nu}, \{B_i\omega_i H^{-\vartheta_i}\}, r, 1) \quad (51)$$

$$= \tilde{F}^+(At(L/r)^{1/\nu}, \{B_i\omega_i (L/r)^{-\vartheta_i}\}, r, 1). \quad (52)$$

The solutions $F^{\pm}$ match at $r = 1, L = H$ and we define the probability for horizontal spanning as $F_h(p, L, r) = F^+$ (F^-) for $r \geq 1$ ($r < 1$). The probability for the vertical spanning F_v is then given by the simple identity [2] $F_v(p, L, r) = F_h(p, L, 1/r) = F^-$ (F^+) for $r \geq 1$ ($r < 1$).

Studying horizontal (or, equivalently, vertical) spanning in two dual lattices and cells of size $L \times rL$ and $L/r \times L$ ($r > 1$, for simplicity) reveals that

$$F^-(p, L, r) + F^+(1 - p, L, 1/r) = 1. \quad (53)$$

Transforming both terms on the left-hand side using the scaling relations [see Eqs. (5) and (6)], we find that

$$\tilde{F}^-(AtL^{1/\nu}, \{B_i\omega_i L^{-\vartheta_i}\}, 1, r) + \tilde{F}^+(-AtL^{1/\nu}, \{B_i\omega_i L^{-\vartheta_i}\}, 1/r, 1) = 1. \quad (54)$$

In what follows it is useful to introduce a new variable $s = \ln(r/r_0)$ [2]. In this paper we always set $r_0 = 1$ because the nonmultiplicative constant in s, $\ln(r_0)$, can be set to zero by the suitable definition of the rectangular system [9]. With this new variable and denoting the probability for the horizontal spanning by F_h, we find

$$F_h(Ax, \{B_i y_i\}, Cs) + F_h(-Ax, \{B_i y_i\}, -C's) = 1. \quad (55)$$

Taking different derivatives all our earlier results emerge at $s = 0$. For $s \neq 0$ we find that $C = C'$ and $F_h - F_h(0, 0, 0) = F_h - 1/2$ is odd in $\hat{x} = Ax, \{\hat{y}_i = B_i y_i\}$ and $\hat{s} = Cs$. Expanding near criticality and $\hat{s} = 0$ we find that

$$F(\hat{x}, \{\hat{y}_i\}, \hat{s}) = \frac{1}{2} + f_0(\hat{s}) + f_1(\hat{x}, \hat{s}) + \sum_i \hat{y}_i f_{2i}(\hat{x}, \hat{s}) + \cdots, \quad (56)$$

where f_0 is odd in $\hat{s}$, $f_1(\hat{x}, \hat{s})$ is odd in $\hat{x}$ and $\hat{s}$,

$$f_1 = \sum_{k,l} \left[\frac{1}{k!l!} \frac{\partial^{k+l} F}{\partial^k \hat{s} \partial^l \hat{x}} \bigg|_{(0,0)} \hat{s}^k \hat{x}^l \right] \text{ with } k + l \text{ odd}, \quad (57)$$

while f_{2i} contains only even powers of $\hat{s}$ and $\hat{x}$.

With this form we can make contact with other recent work on rectangular systems. Cardy [3] argued that the spanning probability for an infinite rectangular system is universal and derived the analytical formula for $f_0(\hat{s})$. His formula for $f_0(\hat{s})$ is indeed odd in s. This fact follows here from scaling, universality, and duality.

Similarly to the case of square systems, the different spanning rules (also studied in [2]) and boundary conditions can change the functional form of the universal function F and therefore also f_0. Therefore for the other spanning rules and boundary conditions f_0 need not to be odd in $\hat{s}$. However, we have just established that for given spanning rule and boundary condition the spanning probability function is a continuous universal function of the scaling variables $AL^{1/\nu}(p - p_c), \{B_i\omega_i\}$ *and* Cs. In principle, by introducing two additional (yet unidentified) scaling variables, which would account for the continuous change in the spanning rules and boundary conditions, the universal spanning probability function could be generalized further.

Due to the extensive recent work [3,2,4], which confirms that f_0 is odd in $\hat{s}$, we are left to verify our form of f_1 in the case of horizontal spanning with free boundaries. With fixed $\hat{s}$, the nth moment scales as

$$\hat{\mu}_n(\hat{s}) \equiv (AL^{1/\nu})^n \mu_n(\hat{s}) \tag{58}$$

$$= g_{n,1}(\hat{s}) + \sum_i \hat{y}_i g_{n,2i}(\hat{s}) + \cdots, \tag{59}$$

where we have introduced universal functions g. For even n, we find that $g_{n,1}$ is even and the $g_{n,2i}$'s are odd functions of $\hat{s}$. For odd n, $g_{n,1}$ is odd and the $g_{n,2i}$'s are even functions. From Eq. (56) we argue that the moment ratios μ_n/μ_1^n depend on $\hat{s}$, but reflect the symmetry between aspect ratios r and $1/r$ through $(\mu_n/\mu_1^n)(\hat{s}) = (\mu_n/\mu_1^n)(-\hat{s})$.

D. Square systems with periodic boundary conditions

Systems with periodic boundary conditions do not possess dual symmetries. If we have a certain configuration of occupied and vacant sites, duality means that if occupied sites span horizontally, then vacant sites do not span vertically on the dual lattice. It is easy to invent a counterexample and show that this does not hold for periodic boundary conditions. Therefore, we have no reason to expect that the spanning probability functions have any particular even or odd symmetry.

However, the generic features are expected to hold. The forms of the spanning probability functions depend on the spanning rule; usually the limit of R at criticality is not equal to p_c, but is a universal number; the sum rules of Sec. III A 1 at criticality also remain valid. The metric factors for two different scaling functions are determined as discussed above and have universal ratios. We can expand near criticality and find

$$F(\hat{x}, \{\hat{y}_i\}) = f_0 + f_1(\hat{x}) + \sum_i [\hat{y}_i f_{2i}(\hat{x})] + \sum_{i,j} [\hat{y}_i \hat{y}_j f_{3ij}(\hat{x})] + \cdots, \tag{60}$$

with universal functions f. At the critical line $t = 0$ the data should scale as

$$F(0, \{\hat{y}_i\}) = f_0 + \sum_i b_{0i} L^{-\vartheta_i} + \sum_{i,j} b_{1ij} L^{-\vartheta_i - \vartheta_j} + \cdots, \tag{61}$$

with universal amplitude ratios $b_{1ij}/(b_{0j}b_{i0})$. Similarly, the scaled nth moment $\hat{\mu}_n = (AL^{1/\nu})^n \mu_n$ is a universal function of $\hat{y}_i$. Finally, the moment ratios μ_n/μ_1^n are universal numbers as $L \to \infty$.

The main advantage of periodic boundary conditions concerns the absence of the finite-size corrections of order $1/L$. Thus the leading term in Eq. (61) should always come from a singular irrelevant field.

IV. NUMERICAL RESULTS AND DISCUSSION

In order to check the theoretical predictions we measured the spanning probability and central moments μ_n for site-bond percolation on a square lattice, using square and rectangular system shapes. We mainly used rule $\mathfrak{R}_1$ and free boundaries. Most of the other possibilities (rules $\mathfrak{R}_0$, $\mathfrak{R}_2$, and periodic boundary conditions) were checked only for the pure site and bond problems.

A. Numerical methods

Numerical data were generated using the hull generating walks, which were first used to generate the percolation cluster perimeters by Ziff *et al.* [21]. The method has been used in studies of the spanning probability by Grassberger [5] and Ziff [7]. In particular, using the hull method, Ziff was able to measure the percolation threshold for the site problem on the square lattice very accurately, $p_c = 0.592\,746\,0 \pm 0.000\,000\,5$ [7]. This result demonstrates the power of this method. We now give a very short account of the hull method (for a more detailed discussion see Refs. [5,7]). We describe the method in the case of the site problem on a square system, but extension to the other connectivities and rectangular shapes is straightforward.

Consider a square cell of size $L_{\max}$ with free boundaries for which the spanning along the vertical direction occurs if there exists a cluster connecting the bottom and the top boundaries. We check if there is such a cluster by a leftward biased walk, starting from the lower left corner of the lattice (see Fig. 1 of Ref. [7] for illustration). One step of the walk is generated by the following algorithm.

(i) Attach a pointer to the NN site on the left-hand side.

(ii) Check the pointed NN site.

(iii) *If the state of the site is undetermined*, then occupy it with probability p and make it vacant otherwise.

(iv) *If the site is vacant*, then move the pointer to the next clockwise neighbor, and go to (ii).

(v) *If the site is occupied*, then move the walker to this occupied site and go to (i).

The walk effectively creates a lattice configuration and checks the spanning simultaneously. In order to make sure that a walk does not terminate before the walker reaches either the top row (sample percolates) or crosses the right edge (sample does not percolate), we have to add a column of vacant sites on the left and a row of occupied sites on the bottom.

The method is easy to implement and it is very fast compared to the traditional Hoshen-Kopelman method [22]. Although restricted to two dimensions, we found the method especially attractive because it is very easy to collect data for the spanning probability at fixed occupancy p as a function of the cell size. Suppose one keeps two variables $x_{\max}$ and $y_{\max}$, denoting the maximum x and y coordinates that the walker has visited.

Then one can record data for all the cell sizes up to $L_{\max}$ as intermediate results of the walks, because if at one instant $y_{\max} \geq x_{\max}$ we know that the cell of size $x_{\max}$ must span.

In its original form the method is perfectly suited only for the rule $\mathfrak{R}_1$, for which we have done most of our simulations. However, by randomly filling the lattice and using the hull method for only checking the spanning [ignoring step (iii) above] one can easily extend the method also for rules $\mathfrak{R}_0$ and $\mathfrak{R}_2$ by doing two walks. First we have to check the spanning along the vertical axis and then do another walk from the left lower corner, trying to turn to the right, in order to check the spanning along the horizontal axis. With the information of these walks we can get the data for all the three spanning rules simultaneously. Here we lose some efficiency by having to fill the whole lattice, but we still get data for all the lattice sizes up to the maximum size as intermediate results of the walks.

The moments were calculated using standard percolation algorithms for generating the derivative $\frac{dF}{dp}$ [10] at fixed cell size L (in this work $L = 20-400$). The method consists of filling the lattice with random numbers, evenly distributed between 0 and 1, and doing the binomial search in p in order to find the value of p for which this particular configuration spans the cell for the first time. For each configuration of the random numbers we started from the initial guess $p = 1/2$ and checked if the configuration spanned at this occupancy (i.e., we declared occupied all the sites with random numbers smaller than p). If the system did not span, we increased p by 2^{-n-1}, where n is the number of the iteration. If there existed a spanning cluster we decreased the trial p by 2^{-n-1}. Repeating this binomial search for 14 times we found that this particular configuration spanned for the first time between p and $p + \Delta p$ with $\Delta p = 2^{-14} \approx 6 \times 10^{-5}$. Our approximation for the "threshold" became $p + \frac{1}{2}\Delta p$. Repeating the same procedure for many (typically around 10^6) configurations, we collected the histogram for these threshold p's, $H(p_i)$, with $p_i = (i + 1/2)\Delta p$. This histogram is proportional to the derivative $\frac{dR_L}{dp}$ [10]. Moments were finally calculated by summing over the histogram $\mu_n \approx \sum_i (p_i - p_c)^n H(p_i)$. This convention automatically takes care of the normalization of the moments by $\sum_i H(p_i) = 1$.

B. Free boundaries

1. *Square shapes with rule* $\mathfrak{R}_1$

We first measured the critical points for selected site-bond problems. In general, there exists a certain critical site occupancy p_c for each fixed bond occupancy x and vice versa. These points $[p_c(x)$ or $x_c(p)]$ form the critical line in the (p, x) plane, connecting the critical point for the site problem $(0.592\,746, 1)$ to the critical point for the bond problem $(1, \frac{1}{2})$.

For simplicity, assume for a while that we measured data with fixed site occupancy p and varied x. The calculations with fixed bond occupancy were treated similarly. As a first step the critical point was then estimated using the data for the derivative $\frac{dF}{dx}$ (or $\frac{dF}{dp}$). From Eq. (40) we find that

$$\mu_1 = \sum_i (x_i - x_c)\frac{\Delta R_L}{\Delta x}(x_i) = \langle x \rangle - x_c \propto L^{-1/\nu} \sum_i a_i L^{-\vartheta_i}. \tag{62}$$

Therefore we could plot the average x, $\langle x \rangle$, versus $L^{-1/\nu-\tilde{\vartheta}}$, adjusting $\tilde{\vartheta}$ until the data fell on a straight line, and extrapolate to $L \to \infty$ in order to estimate the critical point and get some feeling of the leading correction. A straight line was best achieved around $\tilde{\vartheta} = 0.9$, as depicted in Fig. 1 for the site-bond problem with $p_c = 0.75$. It is visible from Fig. 1 that the estimate for the critical point is quite insensitive to the precise value of the effective correction exponent $\tilde{\vartheta}$ and the estimated threshold is the same (within $\pm 0.000\,02$) for $\tilde{\vartheta} = 0.8 - 1$. Resulting estimates for a few critical points on the critical line are listed in Table I.

Using these points as estimates for the critical points, we calculated the spanning probability at (p_c, x_c) as a function of L (see Fig. 2). Figure 2 also displays data for the bond problem on the triangular lattice. All the curves approach 1/2 as the cell size gets large, with the leading correction proportional to $1/L$. We have also studied the site problem on the triangular lattice and the site problem with NN and NNN connectivity on the square lattice, which also yield $R(p_c, \infty) = 1/2$. In particular, the site problem on the triangular lattice has $R(p_c, L) = 1/2$ for all L, similarly to the bond problem on the square lattice [see Eq. (39)]. The fact that the spanning probability approaches 1/2 for all the systems demonstrates that it is a universal number, which does not depend on the lattice

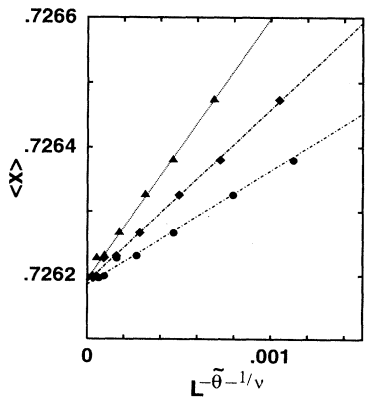

FIG. 1. Average x $[\langle x \rangle = \sum_i x_i \frac{dF}{dx}(x_i)]$ for the site-bond problem with $p_c = 0.75$ versus $L^{-1/\nu-\tilde{\vartheta}}$ for three different values of $\tilde{\vartheta}$: $\tilde{\vartheta} = 0.8$ (•), $\tilde{\vartheta} = 0.9$ (♦), and $\tilde{\vartheta} = 1.0$ (▲). The straight lines are the least-squares fits for the data $L \geq 64$. The extrapolation to $L \to \infty$ gives $x_c = 0.726\,19 \pm .000\,01$ for all the $\tilde{\vartheta} = 0.8, \ldots, 1.0$. Similar behavior was also observed for the other site-bond problems.

TABLE I. Estimates of a few critical points for the site-bond problem. The estimated uncertainty is denoted in the parentheses.

p_c	x_c	
0.5927460(5)[a]	1	(site problem)
0.615185(15)	0.95	
0.667280(15)	0.85	
0.732100(15)	0.75	
0.75	0.726195(15)	
0.815560(30)	0.65	
0.85	0.615810(30)	
0.95	0.533620(30)	
1	0.5	(bond problem)

[a]From Ref. [7].

type or interaction range.

Typical results for the scaled moments $\hat{\mu}_n = L^{n/\nu}\mu_n$ are displayed in Fig. 3. Odd moments indeed vanish faster than $L^{-n/\nu}$, confirming that $f_1(\hat{x})$ is odd. From the same data we also calculated the moment ratios μ_4/μ_2^2 and μ_6/μ_2^3, which are displayed in Fig 4. The leading correction for the moment ratios is proportional to $L^{-2\vartheta_1}$, but the data in Fig. 4 show little dependence on the system size, suggesting that the corrections to scaling are small, as compared to the numerical noise, already for systems with $L > 100$. Averaging the data from systems with $L \geq 140$, we estimate that for the site-bond problems on the square lattice one has $\mu_4/\mu_2^2 = 3.174 \pm 0.025$ and $\mu_6/\mu_2^3 = 17.7 \pm 0.3$ as $L \to \infty$, supporting our proposal that these ratios are universal. Also, as pointed out by Ziff [23], these moment ratios imply that $\frac{dF_1}{dp}$ is not Gaussian. We can compare our results for the moment ratios with Ziff's [23] results for the pure site and bond problems: 3.15 ± 0.05 and 18.5 ± 0.5 for μ_4/μ_2^2 and μ_6/μ_2^3, respectively. Our slightly different result for μ_6/μ_2^3 is presumably due to our larger cell sizes (up to $L = 400$).

Concerning the expansion of the spanning probability function in terms of the scaling variables, it is illustrative to check first the linearized version of the expansion of F,

$$F(x, y_i) = \frac{1}{2} + f_1(\hat{x}) + \sum_i \hat{y}_i f_{2i}(\hat{x}) \approx \frac{1}{2} + \tilde{f}_1(x) + y_1 \tilde{f}_{21}(x) + y_2 \tilde{f}_{22}(x), \quad (63)$$

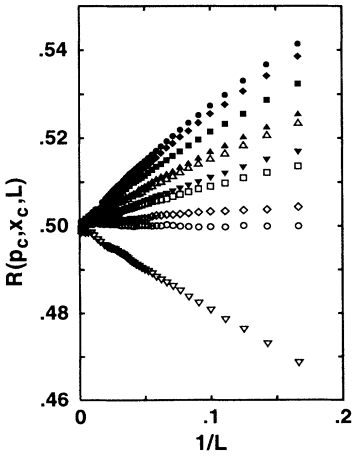

FIG. 2. Spanning probability as a function of $1/L$ for different site-bond problems with spanning rule $\Re_1$. We also show the data for the bond problem on the triangular lattice. All the systems have $F(0,0) = 1/2$. Markers refer to the data for different points on the critical line. From top to bottom: site problem $(p_c, x_c) = (0.592\,746, 1)$ (•), $(0.615\,185, 0.95)$ (♦), $(0.667\,28, 0.85)$ (■), $(0.732\,10, 0.75)$ (▲), $(0.75, 0.726\,195)$ (△), $(0.815\,56, 0.65)$ (▼), $(0.85, 0.615\,81)$ (□), and $(0.95, 0.533\,62)$ (◇); bond problem $(p_c, x_c) = (1, 1/2)$ (○). The lowest data are for the bond problem on the triangular lattice (▽).

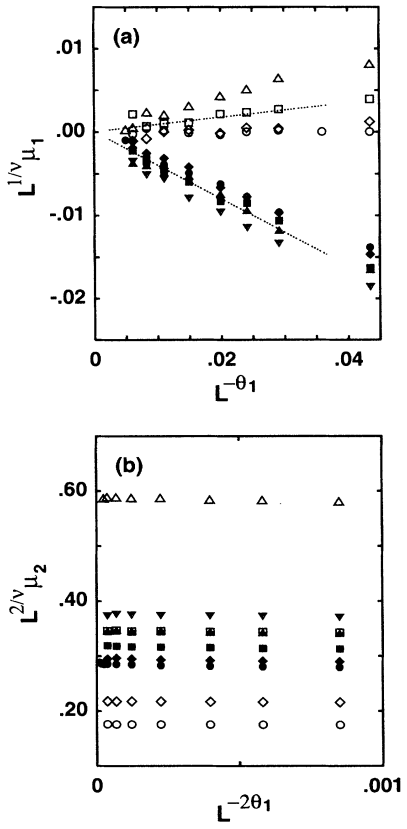

FIG. 3. Typical behavior of the moments for rule $\Re_1$: (a) $\hat{\mu}_1 = L^{1/\nu}\mu_1$ vs $L^{-\vartheta_1}$ with $\vartheta_1 = 0.85$ and (b) $\hat{\mu}_2 = L^{2/\nu}\mu_2$ vs $L^{-2\vartheta_1}$. Markers denote different site-bond problems: site problem $(p_c, x_c) = (0.592\,746, 1)$ (•), $(0.615\,185, 0.95)$ (♦), $(0.667\,28, 0.85)$ (■), $(0.732\,10, 0.75)$ (▲), $(0.75, 0.726\,195)$ (△), $(0.815\,56, 0.65)$ (▼), $(0.85, 0.615\,81)$ (□), and $(0.95, 0.533\,62)$ (◇); bond problem $(p_c, x_c) = (1, 1/2)$ (○). The data drawn with open symbols were calculated keeping the site occupancy fixed and the data represented with filled markers were calculated keeping the bond occupancy fixed. The dashed lines in (a) are only to guide the eye.

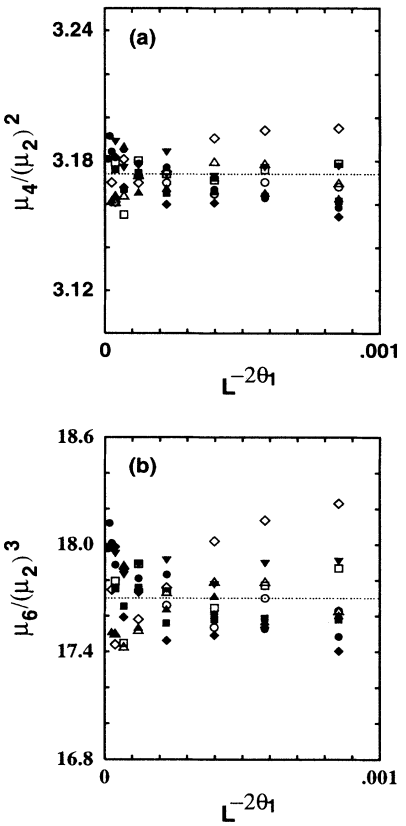

FIG. 4. Moment ratios (a) μ_4/μ_2^2 and (b) μ_6/μ_2^3 versus $L^{-2\vartheta_1}$ for different site-bond problems. Markers are the same as in Fig. 3. The horizontal dashed lines at (a) 3.174 and (b) 17.7 are averages of the data for systems with $L \geq 140$.

with $\vartheta_1 = 0.85$ and $\vartheta_2 = 1$, where the metric factors are appended to the functions $\tilde{f}$. We can project the odd function f_1 out of the data by studying the function $G(x) = \frac{1}{2}[F(x, y_i) + F(-x, y_i) - 1]$. For large L we have

$$G_L(x) \approx \sum_i \hat{y}_i f_{2i}(\hat{x}) \approx L^{-0.85}\tilde{f}_{21}(x) + L^{-1}\tilde{f}_{22}(x). \quad (64)$$

In this respect we have studied only the site problem, for which the data for $L^{0.85}G_L(x)$ and $LG_L(x)$ are shown in Figs. 5(a) and 5(b). In particular, we see from Fig. 5(b) that for $x = L^{1/\nu}(p - p_c) > 1$ the data for $L^{0.85}G_L(x)$ with various cell sizes L collapse well into a single curve. The data collapse is less satisfactory with the analytical correction, which deviates systematically from a common curve [Fig. 5(b)]. Because the analytical correction arises from boundary effects, it is plausible that it vanishes as $\xi \ll L$, where $\xi \propto (p-p_c)^{-\nu}$ is the percolation correlation length. This is satisfied as $x \gg 1$. Therefore, this large x "tail" can be identified as $\tilde{f}_{21}(x)$, whose data collapse confirms the existence of the correction with $\vartheta_1 \approx 0.85$. However, for small x, i.e., closer to the critical axis $t = 0$, the situation is more complicated because there the data show a substantial contribution from the analytical correction, i.e., the function $\tilde{f}_{22}(x)$.

We proceed by fitting a smooth function to the data at $L_0 = 100$, where the data are apparently well described by Eq. (64), and we can ignore the higher-order terms. Using the data for two different system sizes we can eliminate the function $\tilde{f}_{22}(x)$ from Eq. (64) and the function $\tilde{f}_{21}(x)$ should be given approximately by

$$\tilde{f}_{21}(x) = \frac{L^{\vartheta_2}G_L(x) - L_0^{\vartheta_2}G_{L_0}(x)}{L^{-\vartheta_1+\vartheta_2} - L_0^{-\vartheta_1+\vartheta_2}}. \quad (65)$$

Similarly, eliminating the function $\tilde{f}_{21}(x)$, we get the function $\tilde{f}_{22}(x)$,

$$\tilde{f}_{22}(x) = \frac{L^{\vartheta_1}G_L(x) - L_0^{\vartheta_1}G_{L_0}(x)}{L^{\vartheta_1-\vartheta_2} - L_0^{\vartheta_1-\vartheta_2}}. \quad (66)$$

Resulting estimates for the even functions $\tilde{f}_{21}(x)$ and $\tilde{f}_{22}(x)$ are displayed in Figs. 5(c) and 5(d), respectively. Our crude approximations and noise in the numerical data cause a large scatter, but within the scatter we see a reasonable data collapse for our range of system sizes. This supports the form of the expansion near criticality as proposed in Eq. (34).

In particular, Fig. 5 demonstrates that even in the leading order it is necessary to use both the finite-size and the leading irrelevant scaling fields. It is clearly visible in Fig. 5 that the analytic correction is dominant at the critical point and the results are consistent with the analytical prediction $\tilde{f}_{21}(0) = 0$ [see Eq. (22)]. However, the situation is quite the opposite far away ($x > 1$) from the critical point, where the singular correction dominates. As discussed in Sec. III A 2, the fact that $\tilde{f}_{22}(0) \neq 0$ demonstrates that Eq. (22) does not hold for the finite-size corrections for systems that are not self-dual.

From the same data we have checked the prediction (see Appendix B for the derivation) that with a fixed occupancy $p \neq p_c$, the spanning probability $R_p(L)$ depends exponentially on L. The data shown in Fig. 6 confirm this prediction and show in particular that close to p_c and for $L \to \infty$, where the assumptions $L \gg \xi$ and $\xi \propto (p - p_c)^{-\nu}$ both hold, one has

$$R_p(L) = [\tilde{F}_-(1)]^{L(p-p_c)^\nu/\xi_-} \equiv C_-^{L(p-p_c)^\nu}$$

$$\text{for } p < p_c, \quad (67)$$

$$1 - R_p(L) = [1 - \tilde{F}_+(1)]^{L(p-p_c)^\nu/\xi_+} \equiv C_+^{L(p-p_c)^\nu}$$

$$\text{for } p > p_c, \quad (68)$$

where the functions $\tilde{F}_\pm$ are defined in Appendix B and $C_\pm$ are constants as long as the corrections to scaling are ignored. Deviations from the common curves for the data below and above p_c, which are visible in Fig. 6, are due to these corrections to scaling.

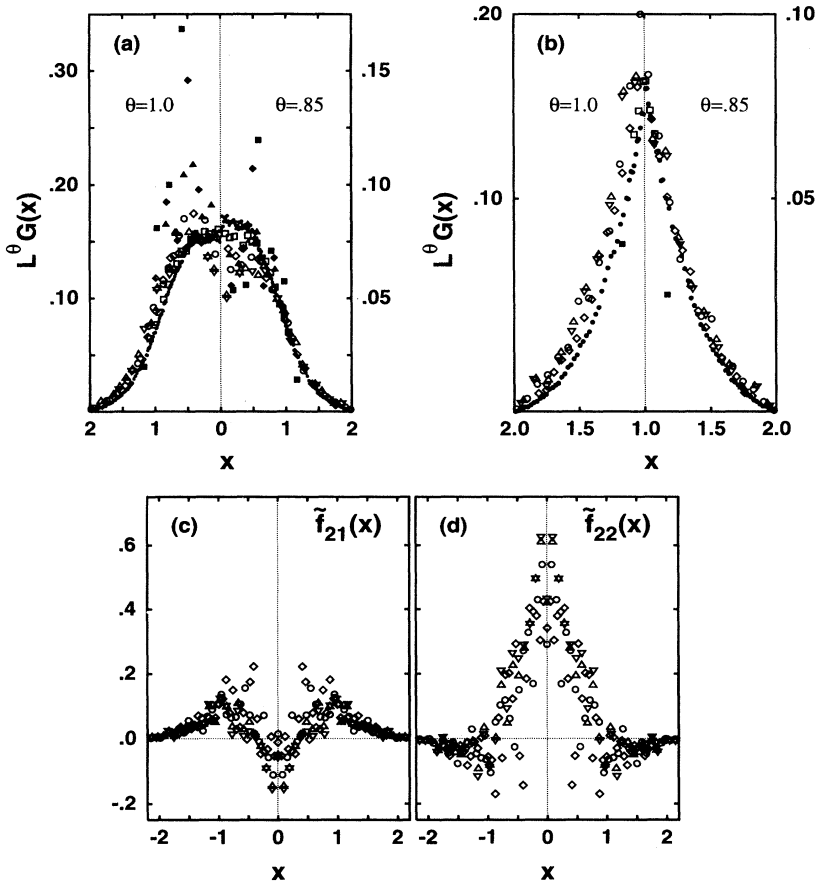

FIG. 5. (a) The function $L^{\vartheta}G_L(x)$ for several system sizes L: $L = 60$ (•), $L = 100$ (□), $L = 200$ (◇), $L = 300$ (○), $L = 390$ (△), $L = 395$ (▽), $L = 640$ (▲), $L = 800$ (♦), and $L = 1000$ (■). The left-hand side has $\vartheta = 1.0$ and the right-hand side is plotted with $\vartheta = 0.85$. For $L < 400$ we studied 10^7 configurations for each p and the data for $L > 400$ were obtained from $2 - 3 \times 10^6$ configurations per given p. (b) Same data as in (a), enlarged for $x>1$. (c) The scaling function $\tilde{f}_{21}(x)$ from various system sizes $400 > L \geq 200$. Data for lattice sizes $L > 400$ have large statistical noise and therefore are not plotted. (d) The scaling function $\tilde{f}_{22}(x)$ from various system sizes $400 > L \geq 200$.

2. *Square shapes with rules $\mathfrak{R}_0$ and $\mathfrak{R}_2$*

This section is devoted to the different sum rules described in Sec. III A 1. For that purpose we have studied only the pure site and bond problems, with the spanning rules $\mathfrak{R}_0$ and $\mathfrak{R}_2$.

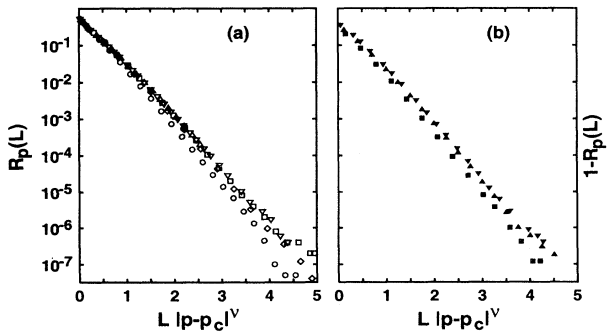

FIG. 6. (a) Data for $R_L(p)$ at a fixed occupancy p below p_c and (b) $1 - R_L(p)$ at p above p_c, for the site problem with free boundaries and rule $\mathfrak{R}_1$. The data for different site occupancies below p_c are represented by open markers: $\Delta p = p - p_c = -0.317\,35$ (○), $-0.199\,375$ (◇), $-0.149\,875$ (□), -0.0924 (△), and -0.0341 (▽). The data above p_c are shown by filled markers: $\Delta p = 0.0341$ (▼), 0.0924 (♦), and $0.149\,875$ (■).

The spanning probabilities at the critical threshold p_c are shown in Figs. 7(a) and 7(b) for the rules $\mathfrak{R}_0$ and $\mathfrak{R}_2$, respectively. We estimate that $F_0(0,0) = 0.6778 \pm 0.0003$ and $F_2(0,0) = 0.3222 \pm 0.0003$, in excellent accordance with the analytical formula from conformal invariance [4], which yields $F_1(0,0) \approx 0.6777$ and $F_2(0,0) = 1 - F_0(0,0)$.

Fitting the data for rule $\mathfrak{R}_r$ at p_c (say, for the range $L \geq 6$) with the expansion

$$F_r(0,\hat{y}_i) = F_r(0,0) + b_r L^{-\vartheta_1} + a_r L^{-\vartheta_2} + c_r L^{-\vartheta_1-\vartheta_2}, \tag{69}$$

where the last term approximates the second-order corrections, gives $b_0 = 0.059 \pm 0.02$ (0.046 ± 0.02), $a_0 = 0.21 \pm 0.02$ (-0.070 ± 0.02), $c_0 = -0.45 \pm 0.05$ (0.36 ± 0.05), $b_2 = -0.050 \pm 0.03$ (-0.035 ± 0.02), $a_2 = 0.41 \pm 0.02$ (0.055 ± 0.02), and $c_2 = -0.17 \pm 0.05$ (-0.38 ± 0.05) for the site (bond) problem. Also for these spanning rules the finite-size correction appears to dominate exactly at p_c, at least over our limited range of system sizes. Although the error bars are large, these fits are reasonably consistent with the prediction that the metric factors of irrelevant fields differ only in sign for rules $\mathfrak{R}_0$ and $\mathfrak{R}_2$ ($b_0 \approx -b_2$) [see Eq. (31)]. Furthermore, fitting the data for rule $\mathfrak{R}_1$, we find the finite-size correction amplitudes $a_1 = 0.31 \pm 0.01$ (0) for the site (bond) problems. Thus we also confirm the prediction that the amplitudes for finite-size correction terms satisfy the weaker sum rule

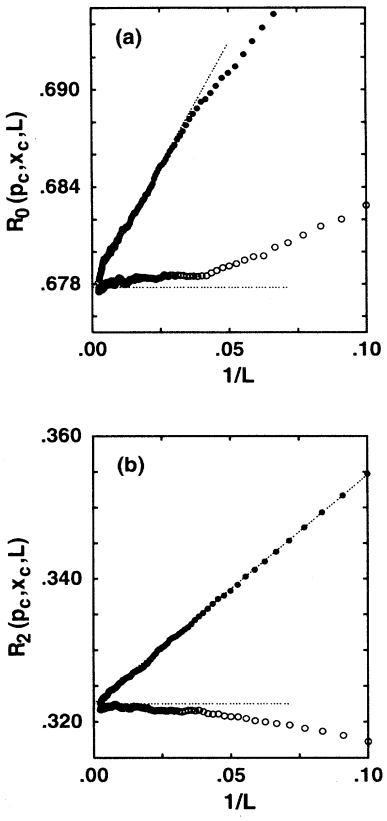

FIG. 7. Spanning probability for the site (•) and bond (○) problems as a function of $1/L$ accoding to the rules (a) $\mathfrak{R}_0$ and (b) $\mathfrak{R}_2$. The dashed lines guide the eye.

$a_0 = 2a_1 - a_2$ [Eq. (11)]. The universal amplitude ratios shall be established for the periodic boundary conditions below.

The first two scaled moments $\hat{\mu}_n = L^{1/\nu}\mu_n$, n=1,2 are displayed in Fig. 8, giving typical examples for the behavior of even and odd moments ($\hat{\mu}_{1,1}$ is already shown in Fig. 3). Comparing the moments for all the rules we observe that $\hat{\mu}$ is rule independent for even n, and $\hat{\mu}_{0,n} = -\hat{\mu}_{2,n}, \hat{\mu}_{1,n} = 0$ for odd n, as proposed in Eqs. (40), (45), and (46). This confirms the sum rule, Eq. (10), and its consequence that all these rules have the same scale factor A. However, A depends on the underlying percolation problem. In Ref. [8] we estimated that the site problem on the square lattice has $A_{\mathrm{sq,site}} \approx 0.765 \pm 0.005$.

The moment ratios μ_n/μ_1^n for rules $\mathfrak{R}_0$ and $\mathfrak{R}_2$ (see Fig. 9 for the data and Table II for the extrapolation results) are found to be the same for both rules and are also the same for the site and bond problems in accordance with the sum rules and universality arguments.

TABLE II. Moment ratios μ_n/μ_1^n for square cells according to the rule $\mathfrak{R}_0$ (ratios for $\mathfrak{R}_2$ are equal) and free boundary conditions.

	$\mathfrak{R}_0$ ($\mathfrak{R}_2$)
$n = 2$	5.53 ± 0.10
$n = 3$	15.7 ± 0.2
$n = 4$	97 ± 2
$n = 5$	435 ± 10
$n = 6$	3010 ± 50

Because even moments $\hat{\mu}_n$ are rule independent due to the duality, the moment ratios μ_4/μ_2^2 and μ_6/μ_2^3 are equal for all the rules. Using the moment ratios from Table II, we find that rules $\mathfrak{R}_0$ and $\mathfrak{R}_2$ have $\mu_4/\mu_2^2 = 3.172 \pm 0.030$ and $\mu_6/\mu_2^3 = 17.8 \pm 0.3$, which are equal to the moment ratios found for the rule $\mathfrak{R}_1$. These distributions are thus not Gaussian and for rules $\mathfrak{R}_0$ and $\mathfrak{R}_2$ they are even asymmetric.

3. *Rectangular systems*

We studied the rectangular cells mainly at aspect ratios $r = 1/2$ and $r = 2$ and with the spanning rule $\mathfrak{R}_1$. Langlands *et al.* have shown that the $L \to \infty$ limit of the spanning function at p_c is a universal quantity [2,4]. Here we present data only for the moments.

The scaled moments for $r = 1/2$ and $r = 2$ are shown in Fig. 10. This figure confirms that $f_0(\hat{s})$ in Eq. (56) is odd in $\hat{s}$ as discussed in Sec. III C. The data also seem to scale well with the leading nonanalytic correction having $\vartheta_1 = 0.85$. The moment ratios μ_n/μ_1^n calculated from the same data are shown in Fig. 11. We find that these

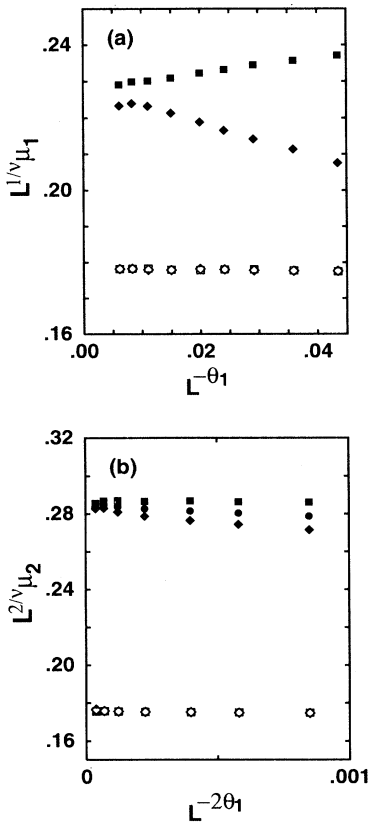

FIG. 8. Typical behavior of the scaled moments for the site (filled markers) and bond (open markers) problems according to the different spanning rules: (a) $\hat{\mu}_1 = L^{1/\nu}\mu_1$ for rule $\mathfrak{R}_0$ (□) and $-\hat{\mu}_1$ for rule $\mathfrak{R}_2$ (◇). The scaled moments for the rule $\mathfrak{R}_1$ vanish at criticality for both systems and are already shown in Fig. 3. (b) $\hat{\mu}_2 = L^{2/\nu}\mu_2$ vs $L^{-2\vartheta_1}$ for the rules $\mathfrak{R}_0$ (□), $\mathfrak{R}_1$ (•), and $\mathfrak{R}_2$ (◇).

TABLE III. Moment ratios μ_n/μ_1^n for rectangular cells with $r = 1/2$ and 2 according to the rule $\Re_1$ and free boundary conditions.

	$r = 1/2, 2$
$n = 2$	2.181 ± 0.005
$n = 3$	4.81 ± 0.03
$n = 4$	13.69 ± 0.10
$n = 5$	41.6 ± 0.3
$n = 6$	145 ± 2

moment ratios are independent of the underlying system and show even symmetry as a function of $\hat{s}$ as predicted in Sec. III C. The universal moment ratios for $r = 1/2$ and $r = 2$ are listed in Table III.

C. Periodic boundary conditions

Due to the lack of dual symmetries, the periodic boundary conditions do not have any particular even or odd symmetry, but possess the generic features of universality as outlined in Sec. III D. Furthermore, due to the more complicated topology, we cannot use the hull generating walk method in its full power, but we have to handle each lattice size separately even for fixed p. However, we expect that for the periodic boundary conditions the next correction to scaling field has $\vartheta_2 \approx 2$, instead of the stronger $1/L$ correction for the free boundaries. Therefore we can study the confluent corrections more accurately.

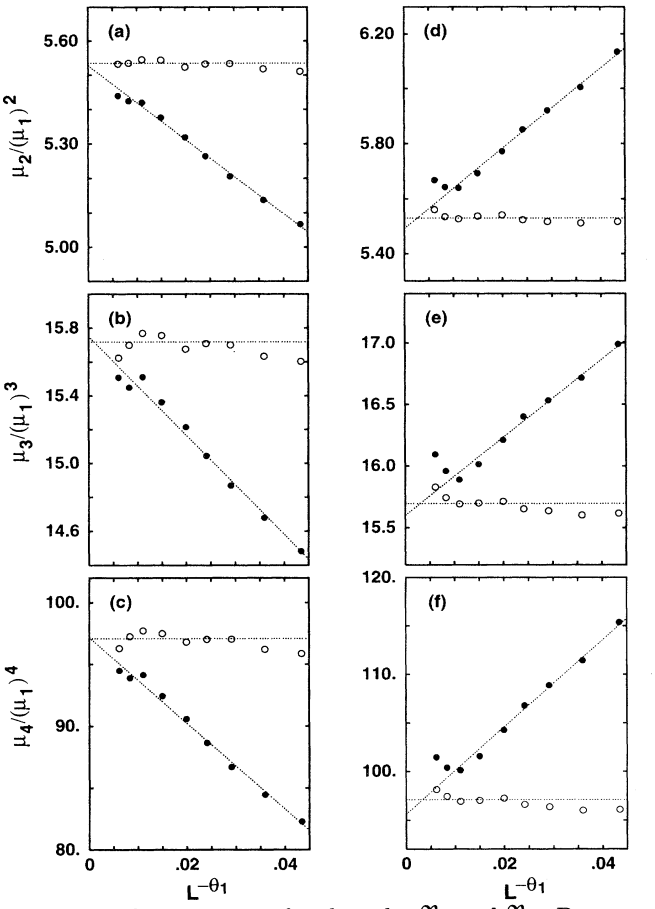

FIG. 9. Moment ratios for the rules $\Re_0$ and $\Re_2$. Data are calculated for the site (•) and bond (○) problems. The left column refers to the rule $\Re_0$: (a) μ_2/μ_1^2, (b) μ_3/μ_1^3, and (c) μ_4/μ_1^4. The right column shows the same ratios for the rule $\Re_2$: (d) μ_2/μ_1^2, (e) μ_3/μ_1^3, and (f) μ_4/μ_1^4. The dashed lines are guides to the eye. For the site problem the lines are linear least-squares fits ignoring the largest ($L = 400$) and smallest ($L = 40$) system sizes. The data for the bond problem with $L \geq 80$ are well described by fixing the correction to scaling amplitude to zero.

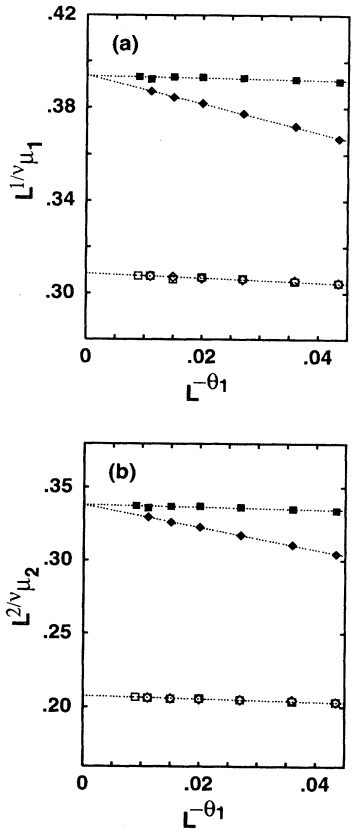

FIG. 10. Scaled moments $\hat{\mu}_n = L^{n/\nu}\mu_n$ as a function of $L^{-\vartheta_1}$, $\vartheta_1 = 0.85$ for rectangular cells with aspect ratio $r = 1/2$ ($\diamond$) and $r = 2$ ($\square$): (a) $-\hat{\mu}_1$ for $r = 1/2$ and $\hat{\mu}_1$ for $r = 2$ and (b) $\hat{\mu}_2$. Open markers are for the data for the bond problem and filled markers refer to the site problem. The dashed lines are linear least-squares fits to the data.

The spanning probability at the critical threshold for the site and bond problems and the three spanning rules are displayed in Fig. 12. Once again, both systems have the same spanning probability at criticality. In order to analyze the data we used the expansion

$$R(p_c, L) = F(0,0) + B_1\omega_1 L^{-\vartheta_1} + (B_1\omega_1)^2 \Delta L^{-2\vartheta_1}, \tag{70}$$

where $\Delta = \frac{1}{2}\frac{\partial^2 F}{\partial \hat{y}_1^2}(0,0)$ is universal, but may differ between different spanning rules, each having its own scaling function. Using straightforward least-squares fits to

Eq. (70) with various ranges of system sizes and extrapolating the resulting coefficients to $L \to \infty$, we find that the spanning probability approaches the universal values 0.814 68 ± 0.0005, 0.636 65 ± 0.0008, and 0.4584 ± 0.0005 for the site and bond problems with $\mathfrak{R}_0$, $\mathfrak{R}_1$, and $\mathfrak{R}_2$, respectively. The general sum rule $F_0(0,0) + F_2(0,0) = 2F_1(0,0)$ is again well confirmed.

In order to establish that for large L the above expansion is adequate, we have plotted $L^{\vartheta_1}[R(p_c,L) - F(0,0)] = a + bL^{-\vartheta_1}$ in Fig. 13. We see that the data fall indeed close to straight lines apart from the large scatter. The amplitudes for the leading corrections can be read from the intercept, giving $a = B_1\omega_1 = -0.29\pm0.02$ (-0.24 ± 0.02), -0.305 ± 0.03 (-0.26 ± 0.02), and -0.325 ± 0.04 (-0.275 ± 0.03) for the site (bond) problem with the rules $\mathfrak{R}_0$, $\mathfrak{R}_1$, and $\mathfrak{R}_2$, respectively. Using the scale factors a_r for different spanning rules we find the ratios $a_0/a_2 = 0.89 \pm 0.04$ (0.87 ± 0.04) and $a_1/a_2 = 0.94\pm0.05$ (0.95 ± 0.04) for the site (bond) problems. The universality between the ratios of the metric factors is apparently well established.

The straightforward least-squares fit using the full expansion

$$R(p_c,L) = F(0,0) + B_1\omega_1 L^{-\vartheta_1} + (B_1\omega_1)^2\Delta L^{-2\vartheta_1} + B_2L^{-2}, \quad (71)$$

which approximates higher-order corrections by the last term, leads to large uncertainties especially for the coefficients of the last two terms. Fitting the data to Eq. (71) for different ranges of system sizes, we estimate $\Delta = -30 \pm 10, -20 \pm 10$, and -30 ± 15 for the spanning rules $\mathfrak{R}_0$, $\mathfrak{R}_1$, and $\mathfrak{R}_2$, respectively. The uncertainties represent numerical difficulties in fitting the

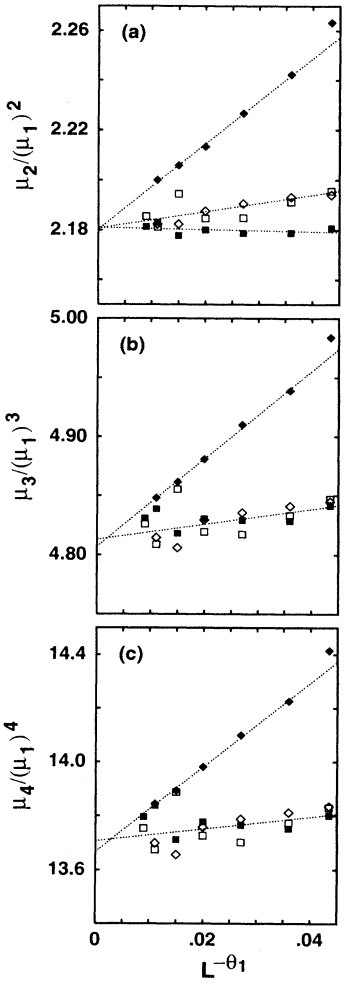

FIG. 11. Moment ratios for the rectangular systems with aspect ratios $r = 1/2$ (◇) and $r = 2$ (□) with the spanning rule $\mathfrak{R}_1$. Data are calculated for the site (filled markers) and bond (open markers) problems: (a) μ_2/μ_1^2, (b) μ_3/μ_1^3, and (c) μ_4/μ_1^4. The dashed lines are least-squares fits to the calculated data.

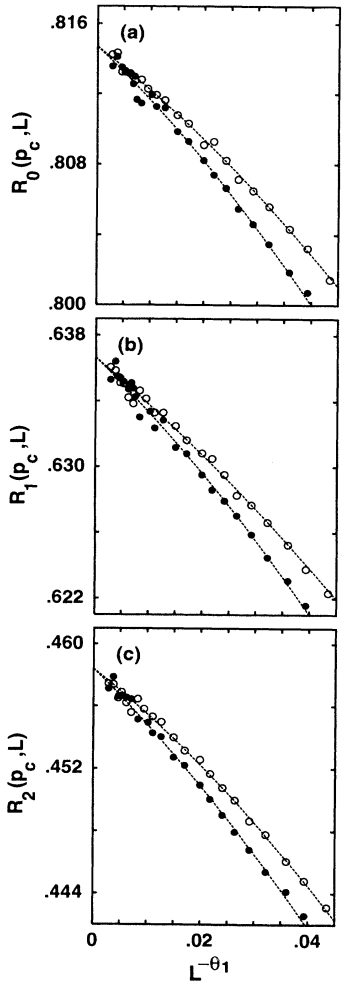

FIG. 12. Spanning probability for the site (•) and bond (○) problems with periodic boundary conditions and for the three different spanning rules: (a) $\mathfrak{R}_0$, (b) $\mathfrak{R}_1$, and (c) $\mathfrak{R}_2$. The dashed lines guiding the eye are typical fits to Eq. (70) using system sizes with $L \geq 50$.

data because the results depend strongly on the range of the system sizes that are taken into account in the fitting procedure. With a fixed range of the system sizes (say, $50 \leq L \leq 1000$), the fitted amplitude ratios are typically equal for both systems within 20%.

The universality of Δ becomes perhaps more convincingly evident from Fig. 14. In this figure we have collapsed the data from the site and the bond problems to a single curve by considering Eq. (71), from which we find that

$$\frac{1}{B_1\omega_1}L^{\vartheta_1}[R(p_c,L)-F(0,0)]$$

$$=1+[\Delta+B_2/(B_1\omega_1)^2L^{-2+2\vartheta_1}](B_1\omega_1L^{-\vartheta_1})$$
$$\approx 1-\Delta(-B_1\omega_1L^{-\vartheta_1}) \text{ as } L\to\infty. \quad (72)$$

Using the estimates for the amplitudes $B_1\omega_1$ as quoted above, Fig. 14 displays the plots of $\frac{1}{B_1\omega_1}L^{\vartheta_1}[R(p_c,L)-F(0,0)]$ vs $-B_1\omega_1L^{-\vartheta_1}$. From this figure it becomes apparent that both systems have the same derivative at the intercept, giving another estimate for the universal amplitude ratio Δ. The agreement with the theory is most convincing for the rules $\mathfrak{R}_0$ and $\mathfrak{R}_1$, but somewhat disappointing for the rule $\mathfrak{R}_2$. This is apparently due to the different signs of the higher-order corrections, represented as a term proportional to L^{-2}. Therefore, Fig. 14 gives strong support in favor of the universal amplitude ratio for the leading irrelevant variable, with $\Delta \approx -25$ for all the rules. Taking these estimates for Δ together with those from the least-squares fits, we quote our final estimate as $\Delta = -25 \pm 5$, independent of the spanning rule. Note that the amplitude ratios need not be equal for

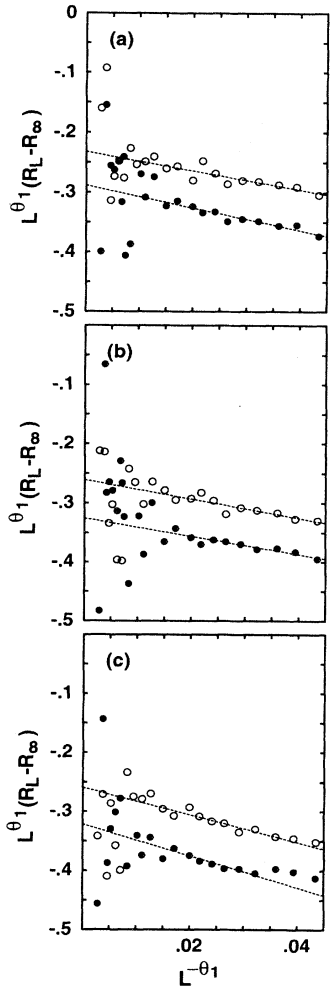

FIG. 13. Same data as in Fig. 12, plotted as $L^{\vartheta_1}[R(p_c,L)-F(0,0)]$ vs $L^{-\vartheta_1}$. The markers refer to the different percolation problems: site (•) and bond (○) problems. Data shown for the three different spanning rules: (a) $\mathfrak{R}_0$, (b) $\mathfrak{R}_1$, and (c) $\mathfrak{R}_2$.

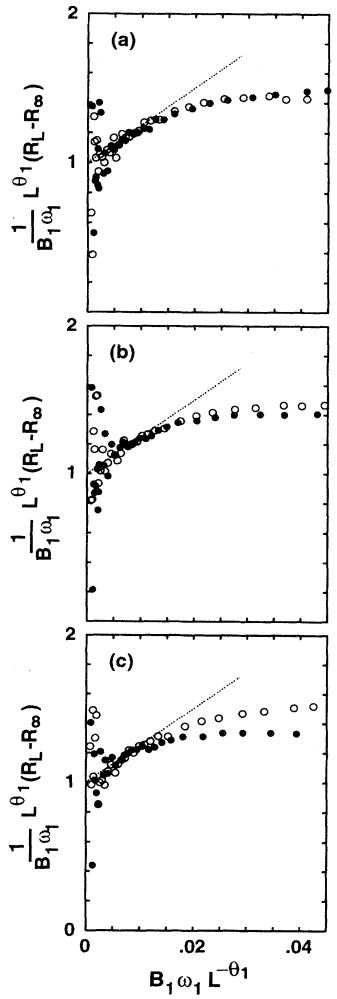

FIG. 14. Same data as in Fig. 13 plotted as $\frac{1}{B_1\omega_1}L^{\vartheta_1}[R(p_c,L)-F(0,0)]$ vs $-B_1\omega_1L^{-\vartheta_1}$ for the site (•) and bond (○) problems. Data shown for the three different spanning rules: (a) $\mathfrak{R}_0$, (b) $\mathfrak{R}_1$, and (c) $\mathfrak{R}_2$. The slope at the intercept gives an estimate for the universal amplitude ratio $-\Delta$. The dashed lines correspond to $\Delta = -25$ for all the rules.

TABLE IV. Moment ratios μ_n/μ_1^n for square systems with periodic boundary conditions with the spanning rules $\mathfrak{R}_0$, $\mathfrak{R}_1$, and $\mathfrak{R}_2$.

	$\mathfrak{R}_0$	$\mathfrak{R}_1$	$\mathfrak{R}_2$
$n=2$	2.259 ± 0.009	9.64 ± 0.20	69.1 ± 2.3
$n=3$	4.99 ± 0.02	26.3 ± 0.4	273 ± 5
$n=4$	14.45 ± 0.10	289 ± 15	15070 ± 700
$n=5$	44.0 ± 0.3	1220 ± 40	$(12.3 \pm 0.7) \times 10^4$
$n=6$	154.3 ± 1.2	15100 ± 900	$(5.9 \pm 0.8) \times 10^6$

all the rules, but it seems that the differences are smaller than our error bars.

The moment ratios μ_n/μ_1^n for the three different spanning rules are listed in Table IV. As an example, extrapolation to $L \to \infty$ is displayed in Fig. 15 for the ratios μ_2/μ_1^2 and μ_3/μ_1^3. We find the same values for moment ratios for both the bond and the site problems.

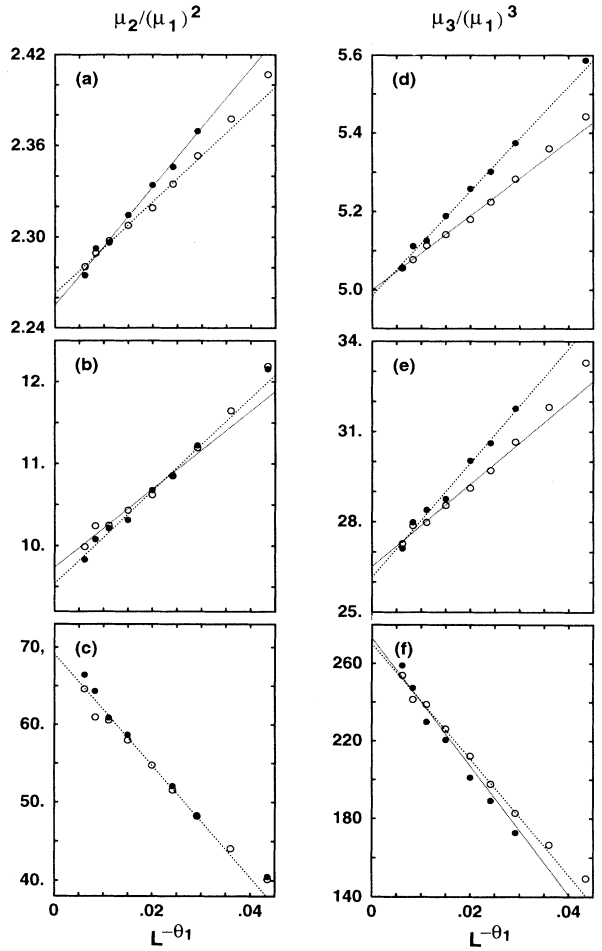

FIG. 15. Moment ratios for systems with periodic boundary conditions and three different spanning rules. Data are calculated for the site (•) and bond (○) problems. The left column refers to the moment ratio $\mu_2/(\mu_1)^2$ for (a) rule $\mathfrak{R}_0$, (b) rule $\mathfrak{R}_1$, and (c) rule $\mathfrak{R}_2$. The right column shows the ratios $\mu_3/(\mu_1)^3$ for the same rules: (d) $\mathfrak{R}_0$, (e) $\mathfrak{R}_1$, and (f) $\mathfrak{R}_2$. The dashed lines are linear least-squares fits for the data $L \geq 64$. (c) contains only one line because the data points overlap.

Note that the moment ratios from Table IV yield $\mu_4/\mu_2^2 = 2.832 \pm 0.025, 3.11 \pm 0.10, 3.16 \pm 0.12$ and $\mu_6/\mu_2^3 = 13.4 \pm 0.3, 16.9 \pm 0.6, 18.0 \pm 2.0$ for rules $\mathfrak{R}_0$, $\mathfrak{R}_1$, and $\mathfrak{R}_2$, respectively. We quote the numbers in order to emphasize that for the free boundary conditions these moment ratios were equal, as a consequence of the duality. This need not be true in general. The moment ratios thus differ for the different spanning rules and boundary conditions. Also for the periodic boundary conditions the distribution is non-Gaussian and asymmetric.

V. CONCLUSION

In this paper we have studied in detail the spanning probability function for three different spanning rules [1], square and rectangular systems, and systems with either free or periodic boundary conditions. Our discussion of the spanning probability function relies on the renormalization group approach, which implies that the scaling functions are determined by the fixed point and therefore universal. It is shown that the renormalization group (scaling) theory, combined with simple relations between the spanning rules and duality arguments, gives strong relations between different derivatives of the spanning function. These relations determine the expansion of the spanning probability function near criticality and give the theoretical background for the numerical work.

Indeed, the theoretical predictions derived from the scaling theory are confirmed numerically with high precision. In particular, we have established the following.

(i) The spanning probability at criticality is a universal number, which need not be equal to p_c, but depends on the scaling function, which is set by the physical question (spanning rules, system shape, etc.) posed at the RG fixed point. This should hold in general d dimensions.

(ii) The scaling variables enter the universal scaling function through nonuniversal metric factors, which can be set by fixing derivatives of scaling functions. The ratios between the metric factors of the irrelevant scaling fields for two different scaling functions are universal. This should also hold in general dimensionality.

(iii) Indeed, we found that the spanning probability is a universal function of $(p - p_c), \{\omega_i\}$'s, *and* the aspect ratio of the rectangular system, apart from the choice of the appropriate metric factors.

(iv) The expansion of the spanning probability function in terms of the scaling variables was theoretically derived and numerically confirmed in the case of free

boundary conditions, which shows strongest symmetry in the scaling variables. In particular, it was established that for two-dimensional percolation with free boundaries one needs to consider two corrections to scaling, which are the leading irrelevant scaling field, scaling as $L^{-0.85}$, and the analytical correction $1/L$. For the spanning rule $\mathfrak{R}_1$, the former contribution was shown to vanish exactly at p_c, in agreement with Ziff's numerical observation [7].

(v) The universality of the scaling function is manifested through the universal amplitude ratios. Universal amplitude ratios were numerically estimated by examining the central moments of the distribution $\frac{dR_L}{dp}$ and by studying the spanning probability function at criticality.

(vi) None of the cases studied in this work yield a Gaussian distribution for $\frac{dR_L}{dp}$.

(vii) The spanning probability at a fixed occupancy and with rule $\mathfrak{R}_1$ depends exponentially on L, for every $p \neq p_c$ and for $L \gg \xi$. We propose that the spanning probability in d dimensions scales as $R(L) = [a_-(p)]^L$ for $p < p_c$ and $[1 - R(L)] = [a_+(p)]^{L^{d-1}}$ for $p > p_c$.

Note added. After we finished this project we received work prior to publication [24] in which $R(p, L)$ is found to be a universal function of the scaled variable $(p-p_c)L^{1/\nu}$, with appropriate scale factors. That result seems to require no corrections to scaling, probably due to the fact that the data were collected only for a single large L, where one may justify setting $\{\hat{y}_i = 0\}$.

ACKNOWLEDGMENTS

J.-P.H. thanks the collective phenomena group at the University of Oslo for their hospitality during the initial stages of this work. The calculations were made possible by generous computer resources from the Center of Scientific Computing, Finland. We also thank D. Stauffer and Y. Saint-Aubin for critical reading of the manuscript, M. E. Fisher for a discussion, and V. Privman for sending useful references. J.-P.H. gratefully acknowledges financial support from the Neste Foundation, the Emil Aaltonen Foundation, and the Foundation of Financial Aid of Helsinki University of Technology. The work at Tel Aviv was also supported by a grant from the German-Israeli Foundation.

APPENDIX A: A COMMENT ON RSRG

The real-space RG of Ref. [1] was based on partitioning the underlying lattice into cells of size b and replacing all b^d sites in a cell of size b by a single supersite. The resulting supersite is then declared occupied if there exists a percolating cluster that spans the cell. Thus the probability for the supersite being occupied within this RG transformation is equal to the spanning probability of the original cell. It is important to note that the RG transformation of Ref. [1] ignores the fact that the true RG involves an infinite number of scaling variables, which are taken explicitly into account in Sec. II.

In the context of the one-parameter approximation one can define the fixed point p^* as the solution of the equation $p^*(b) = R(p^*, b)$. We emphasize that this p^* depends on the scale factor b and one assumes that $\lim_{b\to\infty} p^*(b) = p_c$. Expanding $R(p_c)$ near the fixed point, we find

$$R(p_c) = R(p^*) + \lambda(p_c - p^*) + \cdots, \tag{A1}$$

with $\lambda = \frac{dR}{dp}|_{p^*} = Ab^{1/\nu}$. However, the difference $p_c - p^*$ also scales as $Bb^{-1/\nu}$, so that Eq. (A1) reads

$$R(p_c) = F(0,0) = p^* + AB + \cdots \to p_c + AB \quad \text{as } b \to \infty. \tag{A2}$$

Thus even here it follows that $R(p_c, L \to \infty)$ need not be equal to p_c. However, it is illustrative to observe that the universality of the spanning probability at criticality follows only after the corrections to the scaling are treated systematically.

APPENDIX B: BEHAVIOR OF R FOR $p \neq p_C$

Consider the spanning probability with a fixed occupancy p, $R_p(L)$, and the spanning defined according to the rule $\mathfrak{R}_1$ of Ref. [1] (spanning in one given direction, free boundaries in the other direction). Suppose that $p < p_c$, but close enough to p_c such that $\xi = \xi_-(p_c - p)^{-\nu}$, where ξ_- is the correlation length amplitude. Assume also that $L \gg \xi$. Similarly to Eq. (5), but renormalizing until $b^l = \xi$, we find

$$\begin{aligned} R(p, L) &= \tilde{F}(At, \{B_i\omega_i\}, L) \\ &= \tilde{F}(Atb^{l/\nu}, \{B_i\omega_i b^{-l\vartheta}\}, L/b^l) \\ &= \tilde{F}(A\xi_-^{1/\nu}, \{B_i\omega_i t^{\nu\vartheta_i}\}, L/\xi) \approx \tilde{\tilde{F}}_-(L/\xi), \end{aligned} \tag{B1}$$

where the last step follows by ignoring the corrections to scaling and defining a function $\tilde{\tilde{F}}_-$. Because $\tilde{\tilde{F}}_-(1)$ gives the spanning probability for a box of size ξ, this calculation has reduced the system to the dilute (animal) limit and the system spans if there exist L/ξ spanning boxes connecting the lower and upper terminals,

$$R_p(L) = \tilde{\tilde{F}}_-(L/\xi) = [\tilde{\tilde{F}}_-(1)]^{L/\xi}. \tag{B2}$$

This expression is analogous to the small-p limit because as $p \to 0$ one obviously has

$$R_p(L) = p^L. \tag{B3}$$

Thus we find that with a fixed occupancy $p - p_c < 0$ the spanning probability depends exponentially on L,

$$R_p(L) = [a_-(p)]^L, \tag{B4}$$

where the function $a_-(p)$ behaves as

$$a_-(p) \to [\tilde{F}_-(1)]^{(p-p_c)^\nu/\xi_-} \quad \text{as } p \to p_c, L \to \infty \tag{B5}$$
$$\to p \quad \text{as } p \to 0. \tag{B6}$$

A similar argument holds for $p > p_c$. Renormalizing the system until $b^l = \xi$ and arguing that the system spans unless a line of empty boxes of size ξ connects the right and left terminals (in two dimensions), we find that

$$1 - R_p(L) = [a_+(p)]^L, \tag{B7}$$

where the function $a_+(p)$ behaves as

$$a_+(p) \to [1 - \tilde{F}_+(1)]^{(p-p_c)^\nu/\xi_+} \quad \text{as } p \to p_c, L \to \infty \tag{B8}$$
$$\to 1 - p \quad \text{as } p \to 1. \tag{B9}$$

The corrections to scaling can be taken into account in a straightforward way and the exponential dependence of $R_p(L)$ on L remains unchanged. This prediction is numerically confirmed in Sec. IV for two-dimensional percolation. Furthermore, the argument is easily generalizable to d dimensions, for which one finds that Eq. (B4) remains unchanged, while Eq. (B7) is replaced by

$$1 - R_p(L) = [a_+(p)]^{L^{d-1}} \text{ for } p > p_c. \tag{B10}$$

[1] P. J. Reynolds, H. E. Stanley, and W. Klein, J. Phys. A **11**, L199 (1978); Phys. Rev. B **21**, 1223 (1980).

[2] R . P. Langlands, C. Pichet, Ph. Pouliot, and Y. Saint-Aubin, J. Stat. Phys. **67**, 553 (1992).

[3] J. L. Cardy, J. Phys. A **25**, L201 (1992).

[4] R. P. Langlands, Ph. Pouliot, and Y. Saint-Aubin, Ann. Math. Stat. **30**, 1 (1994).

[5] P. Grassberger, J. Phys. A **25**, 5475 (1992).

[6] J. Bernasconi, Phys. Rev. B **18**, 2185 (1978).

[7] R. M. Ziff, Phys. Rev. Lett. **69**, 2670 (1992).

[8] A. Aharony and J.-P. Hovi, Phys. Rev. Lett. **72**, 1941 (1994).

[9] The rectangular system is a finite cell with aspect ratio r, symmetric with respect to permutation of the two coordinate axes [2]. In particular, the square system has $r = 1$. For lattices that are not intrinsically square, such as the triangular or hexagonal lattices, one needs to choose particular symmetric shapes (e.g., a rhombohedral shape for the triangular lattice) in order to compare with our results.

[10] D. Stauffer and A. Aharony, *Introduction to Percolation Theory*, 2nd ed. (Taylor and Francis, London, 1994).

[11] D. Stauffer, Phys. Lett. **83A**, 404 (1981); J. Adler, M. Moshe, and V. Privman, Ann. Israel Phys. Soc. **5**, 397 (1983).

[12] D. Stauffer, J. Adler, and A. Aharony, J. Phys. A **27**, L475 (1994).

[13] U. Gropengiesser and D. Stauffer, Physica A **210**, 320 (1994).

[14] C.-K. Hu, J. Phys. A **27**, L813 (1994).

[15] D. P. Landau, Phys. Rev. B **13**, 2997 (1976); **14**, 255 (1976); A. E. Ferdinand and M. E. Fisher, *ibid.* **185**, 832 (1969).

[16] C.-K. Hu and J.-A. Chen, J. Phys. A **28**, L73 (1995).

[17] V. Privman and M. E. Fisher, Phys. Rev. B **30**, 322 (1984).

[18] V. Privman, P. C. Hohenberg, and A. Aharony, in *Phase Transitions and Critical Phemonema*, edited by C. Domb and J. L. Lebowitz (Academic, San Diego, 1991), Vol. 14, pp. 1–134.

[19] A. Aharony, Phys. Rev. B **22**, 400 (1980).

[20] A. Aharony and M. E. Fisher, Phys. Rev. B **27**, 4394 (1983).

[21] R. M. Ziff, P. T. Cummings, and G. Stell, J. Phys. A **17**, 3009 (1984).

[22] J. Hoshen and R. Kopelman, Phys. Rev. B **14**, 3428 (1976).

[23] R. M. Ziff, Phys. Rev. Lett. **72**, 1942 (1994).

[24] C.-K. Hu, C.-Y. Lin, and J.-A. Chen, Phys. Rev. Lett. **75**, 193 (1995); **75**, 2786(E) (1995).